Downlink and Uplink User Association in Dense Next-Generation Wireless Networks

APPROVED BY

SUPERVISING COMMITTEE:

Dr. Jeffrey Andrews, Supervisor

Dr. Christine Julien

Downlink and Uplink User Association in Dense Next-Generation Wireless Networks

by

Nikhil Garg

THESIS

Presented to the Faculty of the Cockrell School of Engineering of
The University of Texas at Austin
in Partial Fulfillment
of the Requirements
for the Degree of

Bachelor of Science

THE UNIVERSITY OF TEXAS AT AUSTIN
May 2015

To my parents, for always supporting and pushing me.

To my sister, for keeping me grounded.

Acknowledgments

I would first like to thank my thesis advisor, Prof. Jeffrey Andrews, for his many lessons about research, presentations, hard work, and the field. A little over a year ago, I knew very little about communications. Everything I've learned in the past year has been a direct consequence of his teaching and mentorship. His classes have been among my most challenging and rewarding experiences during my undergraduate education, and his approach to work-life balance has shaped my view of how goal-oriented research should be conducted. I hope to be as effective a mentor and role model as Prof. Andrews. As I proceed to graduate school, I will always keep in mind the lessons I've learned while working with him and his group.

I would also like to thank Prof. Christine Julien for welcoming me into her research group when I was a freshman and for always being there for help and advice. Working in her group helped me stay focused as a young underclassmen and learn how research works. She is one of the most beloved professors in the department, and from her I've learned the importance of listening and addressing students' concerns at a personal level. I hope to be as effective a teacher as her.

I would also like to show my appreciation to other professors in the Wireless Networking & Communications Group (WNCG) and Electrical & Computer Engineering at the University of Texas at Austin. Prof. Yale Patt's enthusiasm for teaching and Computer Architecture has been infectious. He is one of the few teach-

ers I've ever met who can challenge the brightest of students without leaving anyone else behind, and serving as a Teaching Assistant under him taught me the importance of creating structures that help all students succeed. Prof. Caramanis has been a fantastic Senior Design mentor. His flexibility and insistence that the team define its own goals and approach, while facilitating discussions, made for a tremendous experience. I would also like to thank Profs. Brian Evans, Sanjay Shakkottai, Gustavo de Veciana, and Alex Dimakis for their advice and discussions over the years. They constantly reminded me to pursue activities which I enjoy.

I appreciate the opportunity to learn from older students and graduate students in WNCG the past several years. I especially would like to thank Xingqin and Sarabjot for being patient with my questions as I learned about communications research. Mandar, Derya, Abhishek, Qiaoyang, Chang-sik, and Yingzhe have all also been invaluable resources, and I have learned a lot from their comments and discussions. I hope to continue collaborating and meeting with them.

I am grateful for all my friends and family who have made the last four years the most enjoyable of my life. They know who they are and what they mean to me.

Finally, I would like to thank the Plan II Honors program and the Department of Electrical & Computer Engineering at the University of Texas at Austin. Plan II has allowed me to meet and learn alongside a great community of scholars. I would especially like to thank Profs. Galen Strawson, James K. Galbraith, Lee Walker, and Admiral Inman for their insights and lessons.

Downlink and Uplink User Association in Dense Next-Generation Wireless Networks

Nikhil Garg, B.S.
The University of Texas at Austin, 2015

Supervisor: Dr. Jeffrey Andrews

5G, the next-generation cellular network, must serve an aggregate data rate of 1000 times that of current 4G networks while reducing data latency by a factor of ten. To meet these requirements, 5G networks will be far denser than existing networks, and small cells (femtocells and picocells) will augment network capacity. However, dense networks raise questions regarding interference, user association, and handoff between base stations. Where recent papers have demonstrated that interference from small cells will not be prohibitive under multi-slope path loss models, this thesis describes how the use of different path loss models affects the design of such dense, multi-tier networks. This thesis concludes that the gains realized by downlink biasing and uplink/downlink decoupling are strongly dependent on the path loss model assumed and the density differential between base station tiers. Furthermore, this thesis argues that the gains from uplink/downlink decoupling are reduced by a factor of 50% when optimal biasing for the downlink is used.

Table of Contents

List of Tables

List of Figures

Chapter 1

Introduction

1.1 Motivation

Continuing its exponential rise, demand for wireless data services will soon overwhelm existing cellular networks. The success of 4G, 4G LTE, and 4G LTE-A wireless networks has led to a proliferation of mobile apps and novel data uses, including mobile video. Increasing demand comes in two forms: the number of mobile connected devices and the data rate required by each device. In 2014 alone, global mobile data traffic grew 69%, the number of mobile devices grew 7.2% to 7.4 billion, and average data usage on smart phones (the current dominant form of mobile devices) grew 45%, largely due to the spread of LTE [1]. By 2020, overall mobile data traffic is expected to by a factor of ten, and there will be 11.5 billion mobile devices. This number may rise yet further depending on the penetration of Internet of Things technologies. Next generation wireless networks must realize gains on the order of a 1000x increase in transmission capacity and area spectral efficiency to meet this demand [2].

These trends and predictions have informed industry and research targets for 5G networks. These targets include a 1000x improvement in aggregate network data rate and a 100x increase in achievable per-device data rate, from 1 Mbps to 100 Mbps

for 95% of users (all but the worst cell edge users)[2]. These requirements, along with the tentative 2020 goal to implement 5G systems, will outpace the incremental technology improvements in 4G systems, and the entire network architecture must be reimagined for 5G networks.

1.1.1 Network Densification

One of the key ideas toward meeting the requirements is to change the makeup and topology of base stations (BSs). 5G networks will primarily be heterogeneous and multi-tier, taking advantage of multiple Radio Access Technologies (RATs) transmitting at different signal powers on separate tiers; the density of base stations will drastically increase, with density varying by tier [2]. As macro cells become overloaded, it may be beneficial to offload data to dense pico or femtocells in heterogeneous networks. Base stations on smaller tiers, with lower transmit powers and potentially different propagation characteristics, are far more numerous than macro base stations. This offloading trend has already started: 46% of mobile data traffic was offloaded to WiFi or cellular femtocells in 2014, blunting some of the growth of cellular data traffic [1]. This offloading has reduced load on macro base stations and has prevented network overload.

Densification is not new; it has been the key driver of increasing wireless network capacity in the last fifty years [3]. Physical layer improvements have been vital in increasing data rate, and research in that area will continue to drive improvement with respect to metrics such as energy efficiency and latency [4]. However, the increase in system capacity has largely been due to adding base stations. Figure 1.1

charts the contributions of more spectrum, frequency division, modulation & coding, and spectrum re-use due to densification toward increasing system capacity in the last 60 years. This thesis assumes this trend will continue and that network densification will be an important enabler of system capacity increases in 5G networks.

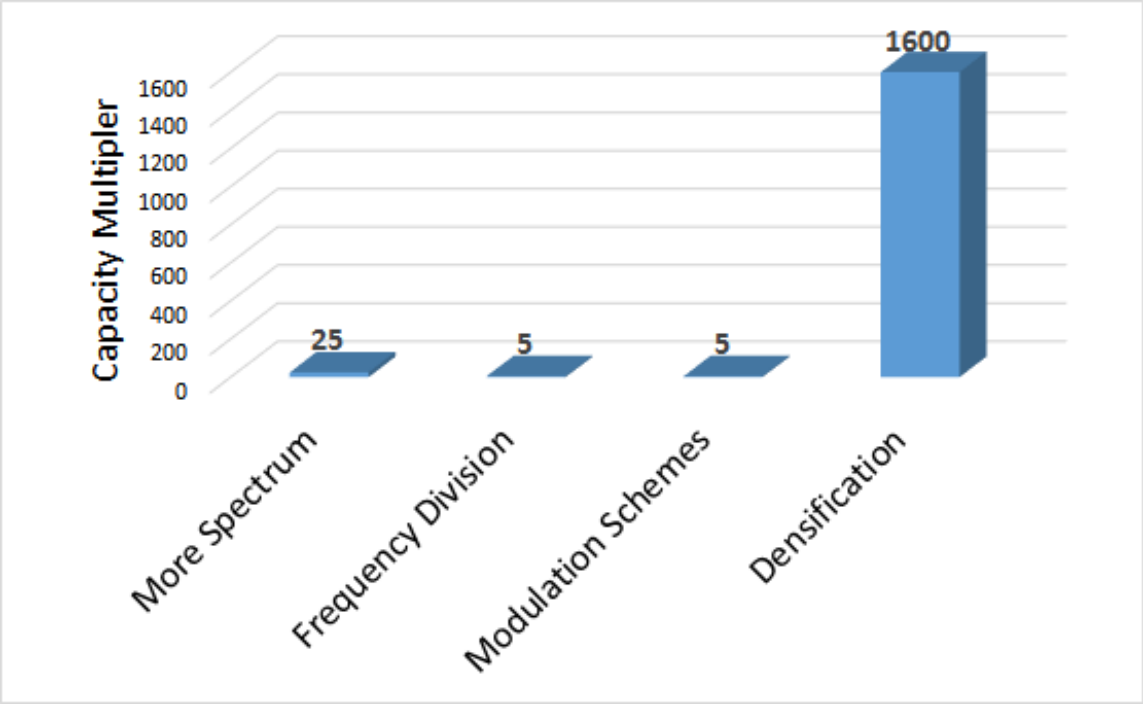

Figure 1.1: Capacity contributions of various factors since 1955 [3]

Several questions remain regarding the ultra-dense networks of tomorrow, including: (a) Is an asymptotically linear throughput gain with increasing density possible, and how will interference be managed to achieve it? and (b) How will network nodes work together to balance load and associate users? These questions drive this thesis and related work. In the following sections, this work's approach and specific questions are made clear.

1.1.2 System Level Modeling

The questions in Section 1.1.1 cannot be answered using traditional information theory. Much of information and communication theory, following the work of Claude Shannon in [5], has focused on deriving bounds for single-link capacity. However, this approach has its limitations: it cannot evaluate the trade-off of evaluating more network nodes at a system level, as adding nodes strictly increases interference and thus decreases link-level capacity. Similarly, it is intractable to use link-level interactions to answer network design questions regarding interaction between multiple base stations, such as how to use biasing to offload users to a lightly loaded cell. Models such as the Wyner model can be used to approximate SIR and SINR at the system level. However, such models require calculations across large grids, with approximations for User Equipment (UE) locations. They do not easily yield distributions for user SIR or SINR. Finding such distributions in the past have required building systems and running large simulations.

However, recent work has introduced the use of stochastic geometry to produce tractable and tight bounds on system level performance [6]. This framework has been used to show that, under dual-slope path loss models with empirically justified path loss exponents, SINR converges to a positive, constant value with increasing network density [7]. Thus, adding nodes (even randomly without sophisticated network planning), asymptotically increases system throughput.

This thesis extends this work to study network design in dense heterogeneous networks. The impact of dual-slope models on the gains realized by biasing and decoupling the uplink from the downlink is studied. Simulations were built to inform

future analytic work.

1.2 Thesis Overview

This thesis seeks to answer questions about user association (for both the uplink and downlink) in dense multi-tier networks using various path loss models. It starts with an overview of wireless performance increases in the last several decades and then previews requirements and technologies in 5G networks. This overview is meant for a lay audience. It then discusses literature and current techniques in user association for both the downlink and uplink and describes the system model and simulation setup. Finally, this thesis poses and answers several questions regarding how different path loss models affect the gains realized by user association techniques.

1.2.1 Chapter Descriptions

In Chapter 2, an historical overview of the technologies and performance of past wireless systems is given, along with projections of required system performance through 2020. Descriptions of some of the key drivers of these performance requirements (the Internet of Things, virtual reality applications, and vehicular networks) are then given. Finally, an envisioned network architecture is described with previous work in user association and heterogeneous networks.

In Chapter 3, the system model is described. Stochastic geometry models are briefly discussed and then the parameters and assumptions used in this thesis are detailed. Finally, the performance metrics used to compare user association strategies are included.

In Chapter 4, the simulations and code flow is described, including the data processing workflow. The simulator is verified by comparing its output to analytic and simulation results from [7]. Benchmarks comparing the C++ code to Matlab code are given. The C++ code is shown to be about 20 times faster than Matlab code.

In Chapter 5, various experiments are described alongside their results. First, the use of static biasing is studied. Optimal bias values for various system design parameters – tier density and power disparities – and for different path loss models are included. Next, uplink/downlink decoupling is studied for various path loss models and downlink association techniques.

1.2.2 Contributions

This thesis answers several questions regarding downlink and uplink user association with different path loss models: a) how does the use of various single and multi-slope path loss models affect the gains predicted for optimal biasing in the downlink? b) what do the different path loss models predict about the gains realized by decoupling the downlink from the uplink? and c) do gains predicted for uplink/downlink decoupling extend to the case when optimal biasing is used for the downlink?

Simulations show that though biasing leads to large gains for a basic single slope path loss model with $\alpha = 2$, these gains are much smaller for larger path loss exponents. Furthermore, both the optimal bias and the gain from biasing is shown to be a function of the relative densities between the tiers. As the relative density for the small cell tier approaches infinity, the gains from biasing tend to zero.

Next, this work quantifies the gain from uplink/downlink decoupling over coupled association with optimal biasing for the downlink. It is shown that there is a small, positive gain from decoupling, but this gain is about 50% less than the gain over coupling without optimal biasing.

Finally, the simulations suggest a possible heuristic that can be used instead of schemes in which the base stations calculate their bias. It is shown that association with optimal biasing can be roughly approximated by a user-centric association in which UEs connect (for the downlink) to the base station that maximizes a linear combination of downlink and uplink SINR. Such an association provides a balance between connecting to small cell BSs (that are lightly loaded) and connecting to the macro BS which may provide the highest downlink power. This scheme can be analyzed in future work.

Chapter 2

5G Overview

2.1 Performance Requirements

Wireless technology has penetrated every aspect of our lives in the last twenty years, and its growth has been staggering. The majority of people in the world now own mobile devices, and adoption of 4G and 4G LTE is increasing worldwide. Each new generation of cellular technology (from 2G through 4G-LTE) has enabled a new type of application. Most recently, 4G-LTE has enabled mobile streaming video and video chatting, which as of 2014 utilizes 55% of mobile data traffic [1]. This section, meant for a lay audience, traces the history of wireless and cellular technologies through the performance of various systems and the usage over time.

2.1.1 History

Figures 2.1, 2.2, 2.3, and 2.4 show historical and projected approximate data rates, total mobile devices, worldwide mobile data traffic, and network latency, respectively, starting from 1940. The data for these figures were collated from [1], [2], [8], [9], [10], [11], [12], and [13]. Note that the 1990s served as an inflection point: the number of global mobile devices, data rates, and total network all increased dramatically, and network latency fell significantly. Since then, there has been an exponential growth in network usage. The 2000s did not see as large of an expo-

nential growth as the 1990s in the number of mobile devices because the mobile cell phone market saturated. However, data usage rose exponentially due to the rise of smart phones. This exponential growth is expected to continue as new applications demand ever-increasing amounts of data.

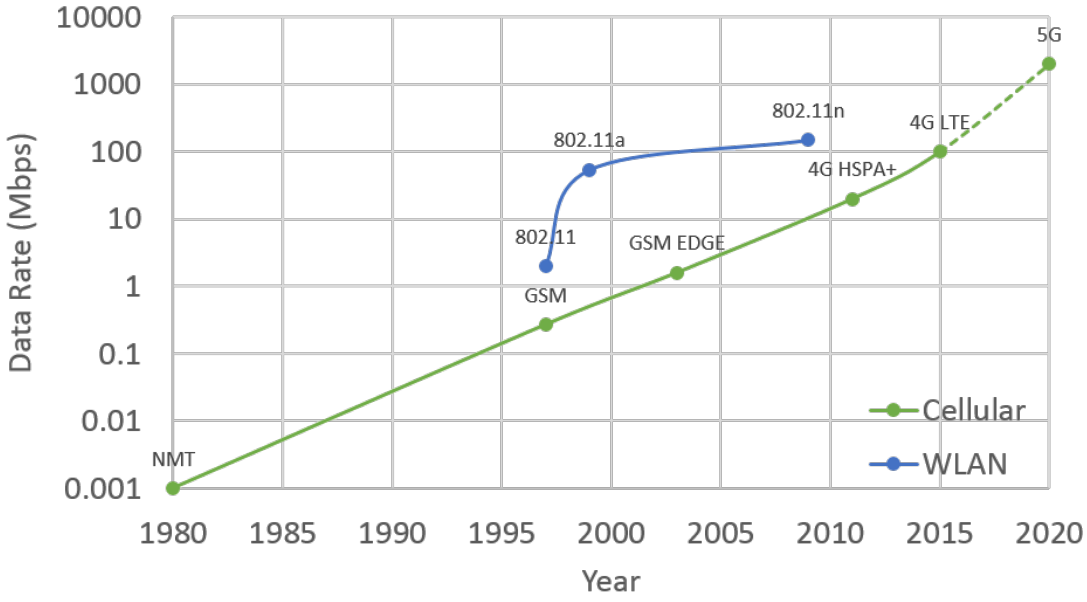

Figure 2.1: Approximate, peak date rate over time for wireless technologies. Exact values depend on network load, location, and distance to the base station, among other factors.

2.1.2 5G System Requirements and Performance Drivers

Driven both by technical feasibility and potential applications, there is a broad consensus on system requirements and goals for 5G [2, 14]. A key aspect of 5G networks is heterogeneity: in both the potential applications and their requirements. 5G networks must support an edge rate 100 Mbps, between 1000x and 10000x more

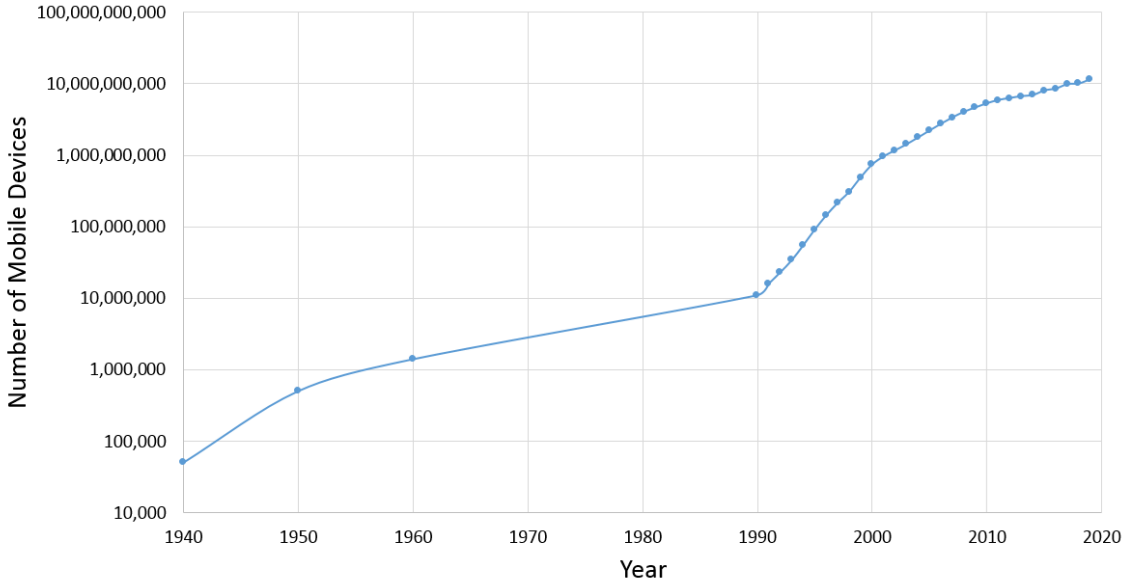

Figure 2.2: Number of mobile devices over time. The 1990s saw a large exponential rise in devices. This rise has tapered in the last five years as the mobile cell phone market has saturated. The IoT market may again lead to an exponential rise, however, by 2020.

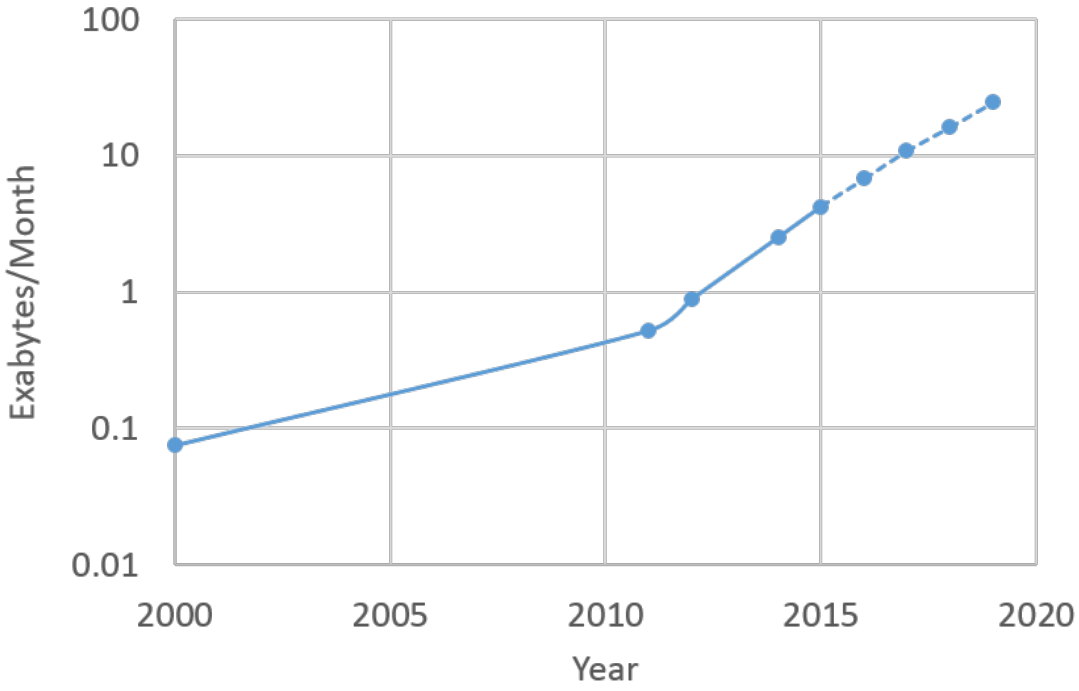

Figure 2.3: Worldwide data traffic over time. While the number of devices has not seen the same exponential rise as it saw in the 1990s, overall data traffic has continued its exponential trend as per device usage has risen.

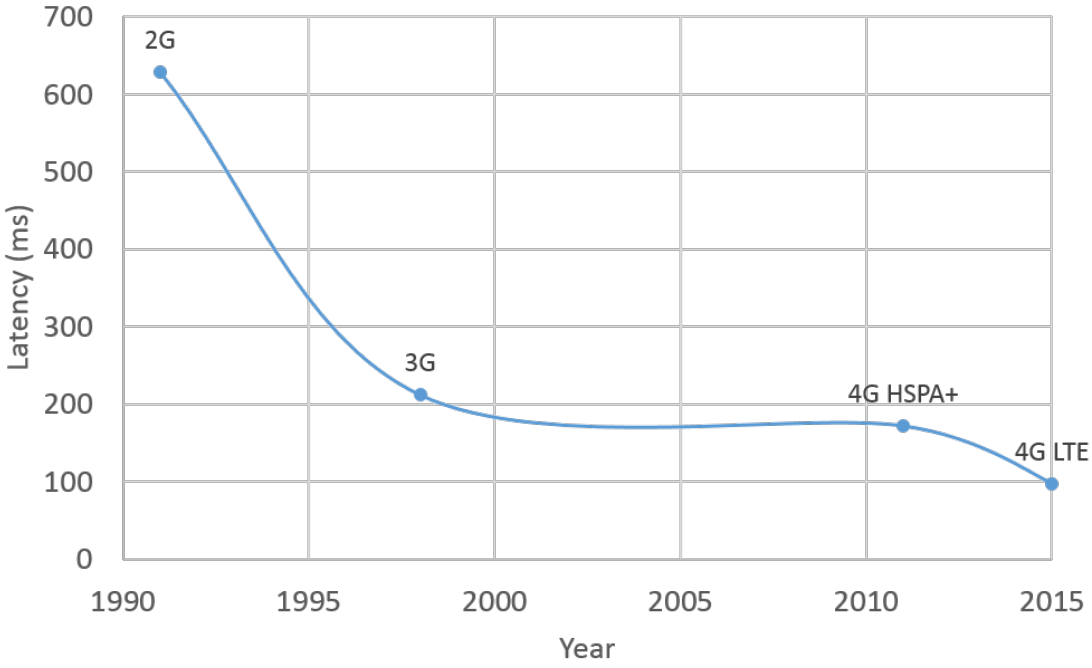

Figure 2.4: Cellular network latency over time, measuring the time it takes to send a packet from a source to a receive through the entire network stack. Note that this time includes not just the link latency (from the base station to a UE), but also the backhaul and internet latency. Drastically lower latency is required for 5G technologies to support new generations of applications.

overall traffic, 1 ms link latency, and high reliability. Some applications, especially sensor networks, will require high uplink capacity. In the following subsections, some of these potential applications are described along with their associated network needs.

2.1.2.1 Internet of Things

One of the largest sources of data and device growth in the next decade will be from "Internet of Things" (IoT) technologies. Though the hype has grown faster than the technology in the last decade, the vision remains the same: "sensors and actuators blend[ing] seamlessly with the environment around us, [with] the information shared across platforms in order to develop a common operating picture" [15]. Market penetration of IoT technologies will strain existing wireless networks. A large number of devices will demand both high downlink and uplink capacity.

One of the most prominent examples of a ready-for-market IoT technology is Nest's home automation technology [16]. Nest builds thermostats, among other devices, that learn when a home is occupied and then optimize the home's heating and air conditioning to save electricity while keeping its occupants comfortable. The technology senses the environment (a regular home, in this case), uploads the data, processes it (often through machine learning techniques), and then controls the environment. Nest, as an indoor technology often meant for homes and businesses, uses WiFi. Future IoT applications, especially those meant for outdoor use, must have cellular capabilities.

Such technologies may soon be ubiquitous, with infrastructure monitoring,

internet search for the physical world, and pervasive sensing. IoT will bring significant economic gain: Cisco estimates that IoT will be a $19 trillion industry by 2020 [17], and Google recently acquired Nest for $3.2 billion [18].

However, significant technological gains must be made to serve IoT applications and sensors. Several architectural challenges remain at the higher layer of the networking stack, including security and the question of how to address the potentially trillions of tagged physical objects [15, 19, 20]. There are several challenges for the wireless communication layers as well. Most fundamentally, there must be enough capacity to connect all networked devices to the core internet, and this capacity will primarily come through densification of the network. The large number of devices also poses challenges in user association, load balancing, and scheduling.

Furthermore, sensor networks will increase demand for wireless uplink capacity. In existing cellular networks, there is much higher demand for the downlink than the uplink. For instance, users stream videos to their device through LTE far more often than they upload videos or other data from their devices. Many architectural decisions (such as uplink/downlink coupling) are based on this assumption. Sensor networks, with non-user devices, turn that relation on its head: any given device only needs to download control or synchronization instructions but needs to continuously upload collected data. The network architecture must evolve to increase uplink capacity without sacrificing downlink capacity.

Finally, parts of the IoT will demand low latency and high reliability connections. Industrial control systems, in particular, are currently only operated through wired networks due to their high reliability and low latency constraints [21]. How-

ever, it may be desirable to run such systems through a wireless network to simplify adding new actuators or sensors and to control systems across a large geographic region. Wireless protocols with low latency at a high reliability must be developed and implemented in 5G network. These IoT challenges must be tackled directly in future cellular network design.

2.1.2.2 Vehicular Networks

The cell phone helped kill the car phone. In the next decade, however, vehicles will be re-connected to the network, but not for human communication. Vehicular networks will come in two forms: Vehicle to Vehicle (V2V) and then Vehicle to Base Station. These networks demand spectrum resources and low latency protocols.

V2V networks are a form of Mobile Ad-Hoc Networks (MANETs) with a long research history. V2V networks involve short range, direct connections between vehicles, often for safety applications. For example, a vehicle could send message to the vehicle behind it that it is suddenly braking, and the trailing vehicle could start the breaking process faster than person at the wheel could respond. The United States is considering mandating that all vehicles manufactured as soon as 2017 have such capabilities [22]. Such communications require very low latency, but V2V in general will not affect 5G cellular design: such networks can be separate from the larger network on their own bands.

However, the second class of vehicular networks, in which vehicles are connected to the larger network, will affect 5G design. Many commercial vehicles already connect their vehicles for tracking purposes. Especially as more autonomous vehicles

enter the marketplace, it will be beneficial to connect more vehicles to the network for control and monitoring purposes. A centralized controller could optimize vehicles' routes through traffic. In a truly autonomous-driving world, such networks will be required for safety and control and could be used to optimize traffic signals [23]. To connect vehicles to the larger network, 5G networks must be able to handle millions of new devices, and much of the communication must be low latency. Furthermore, because vehicles by definition are often moving, low network latency must be preserved even with handoff between base stations.

2.1.2.3 Other Drivers

In addition to IoT and vehicular communication – which require the network to support billions of new devices, high uplink capacity, and low latency – other applications will tax the network with respect to more traditional network performance metrics. For example, augmented reality applications will require large downlink capacity and data rates. Such applications will continually overlay information about the world on devices such as smart glasses.

2.2 Network Heterogeneity

The requirements in Section 2.1 – very large number of devices, high uplink data rates, low latency, and high reliability – are difficult to achieve individually, and all trade off from one another. To meet these requirements, 5G networks will display two types of heterogeneity.

First, different RATs must be coordinated and used. A single wireless tech-

nology cannot meet all the constraints for any given application, and a device may require various types of connections at different times. Devices must be able to simultaneously use different technologies to meet all their needs. For instance, an industrial controller (with sensors and actuators) may need low latency and high reliability for regular operation. It may also occasionally need to upload data that it has collected, thus requiring a high data rate connection; however, a protocol optimized for high reliability with low latency may not support high uplink data rates. These protocols must co-exist.

Furthermore, different technologies can be used to augment cellular technology. For example, WiFi can be used alongside cellular to provide high data rates for stationary or slow-moving users. Various cellular physical layer technologies may also be used together to meet needs; 5G networks will use mmWave, for instance, and machine to machine communication may also be used [2]. This coordination is not always trivial. A fierce debate is currently raging over the use of LTE on unlicensed bands (the 5 GHz band in particular) currently used by WiFi [24–27].

Second, even assuming a single RAT throughout the network, 5G networks will be heterogeneous with respect to transmit power and size of base stations. Traditional cellular towers, or macro base stations, will be supplemented with small cell base stations with lower transmit power. These small cells can augment system capacity by allowing macro base stations to offload some of their users to the smaller base stations. This thesis primarily concerns this type of heterogeneity, and user association and uplink/downlink decoupling are studied with multiple tiers of base stations.

2.3 Network Densification

Along with being heterogeneous, 5G networks will also be asymptotically dense, with femtocells potentially every ten square meters in some geographic areas. Small cells can be installed at a much cheaper cost than can macro base stations. At such a high density, cell edge users are eliminated – all UEs are close to a base station.

2.3.1 Interference in Dense Networks

With such a large number of base stations installed in an unorganized manner, interference can become an issue. Densifying the network makes spatial frequency reuse difficult because unless the bandwidth is split into many orthogonal sub-bands, interfering base stations will be nearby even with frequency reuse. Similarly, sectoring may not be feasible with such small cells due to side lobe leakage. In [7], Zhang and Andrews derived coverage and SINR bounds in a dense network when dual-slope (or more generally, multi-slope) path loss models are used. They found that the scaling on coverage and capacity depend on the path loss parameters: for $\alpha_0 > 2$, the probability of coverage approaches a constant value above zero as density tends to infinity, and so system throughput scales linearly. With $\alpha_0 < 2$, however, the probability of coverage tends to 0 and so system throughput no longer scales linearly. For $\alpha_0 < 1$, system throughput tends to 0 as the density increases. This thesis extends this work to multi-tier networks with a power differential between the tiers and with various user association strategies.

2.3.2 Downlink User Association

Many of the benefits of dense networks may not be realized if users do not connect to the small-cell base stations. In most existing cellular systems, users connect to the base station based on signal strength (SINR). However, users often receive the strongest SINR from macro base stations, rather than from closer, less powerful base stations. The macro base stations may become overloaded, and adding femtocells may not improve network capacity.

In [28], the authors set up a test bed of a dense WiFi network, with two tiers in the 2.4 GHz and 5 GHz bands, respectively. They found that when clients were free to associate to any router in this dense network, they often chose poorly. Router load and resource differences between the bands often led to much higher performance in the 5 GHz band. However, clients often connected to a lower performing 2.4 GHz router because it delivered a higher SINR due to propagation behavior through walls. The overall network capacity, as well as per-user rate for users in the 2.4 GHz band, was lower as a result.

This loss can be recovered by changing user association algorithms. One common user association techniques is to bias users towards lightly loaded tiers. For user association purposes, a biasing factor B_i is added to the received signal power for tier i to extend the range of the tier in the network. In [29], the authors analyze coverage and rate (for the downlink) when biasing is used. They observe that the effect of biasing depends on the bias factor, the relative densities of the network tiers, and on other network specific factors. However, in general, biasing slightly diminishes probability of coverage in exchange for increasing overall rate through

better resource management. In this thesis, simulations show that biasing is further dependent on the path loss model used and, for large densities or higher path loss exponents, the gain from biasing is negligible.

While well-designed biasing may improve performance, static bias factors B_i may not be well suited for dynamic networks (as heterogeneous networks naturally are, as routers may be added or removed without warning). Changing these biases per network configuration may lead to too much overhead. Furthermore, while the factors may be designed based on average or predicted loads on particular tiers, they may be ineffective for instantaneous or actual user distributions in a network. Recent work has sought to dynamically adjust these weights in a distributed and real-time manner [30, 31].

Iterative, distributed algorithms to determine bias weights are used in [30] and [31]. Though the details differ, in both methods base stations broadcast their current biases to users, who use those biases and channel information to tentatively associate with a base station. Each base station then updates its bias based on the number of users connected to it. This process continues until associations converge. Associations are updated as needed, with user mobility or with new users in the system.

2.3.3 Uplink/Downlink Decoupling

The association techniques described above are currently solely used to maximize downlink performance. However, the uplink is considered increasingly important for anticipated applications (especially sensor networks, IoT, and autonomous

vehicles). Recent literature has emphasized large potential gains in the uplink by decoupling user association in the downlink and uplink [32, 33]. The idea of uplink/downlink decoupling is that though connecting to a macro cell may be beneficial in the downlink due to the larger transmit power, the larger distance (higher path loss) hurts uplink SINR. The analysis becomes trickier with uplink power control and downlink biasing, and this work simulates such configurations.

In [32], the authors observe significant throughput gain in the uplink through decoupling the uplink and downlink. Their model includes neither power control nor load balancing for either the uplink or the downlink, and instantaneous channel effects are not considered. Rather, each device connects to the base station from which it receives the highest average power for the downlink and the base station to which it transmits the highest average power in the uplink.

In [33], the authors simulate a dense HetNet using a ray tracing prediction model, yielding detailed performance information. Uplink and downlink association in the decoupled case is similar to above. Downlink association is determined as in LTE (signal power of a reference signal), and uplink association is determined by the path loss to the base station. Through their detailed simulations, the authors also observe significant throughput gains for the uplink through decoupling.

The works described above do not factor in load balancing (for either the uplink or the downlink). In [34], Singh, et. al claims that, without decoupling, biasing for load balancing in the downlink would also benefit the uplink; biasing for the downlink reduces the impact of unequal base station transmit power, and so users are more likely to connect to closer, low power base stations that also exhibit less uplink

path loss. Such a benefit does not negate the benefit from decoupling: the authors in [35] posit that the decoupled uplink would still outperform coupled association with downlink biasing. In this work, simulations show that uplink/downlink decoupling does lead to gains over optimal static biasing for the downlink, but this gain is very small compared to the gain over no biasing for the downlink.

A minimum path loss association is shown to be optimal for the uplink in [34], regardless of power control or network density. However, such an association is optimal with the assumption that such it would lead to an identical load distribution across all APs. While this is true in expectation (with UEs and BSs distributed according to a PPP), it may not be true instantaneously. Rather, for a particular realization, load may be distributed unevenly across the BSs with minimum path loss association. With non-PPP distributions for users (such as clustered users), load may also be quite unbalanced even in expectation. Thus, real-time distributed load balancing for the uplink, similar to that used for the downlink in [31], may increase rate. Future work could extend the results from this thesis which shows the gain from decoupling when constant, static biases are used at each base station across a tier.

This thesis uses a channel inversion path loss model when analyzing uplink capacity, following literature. A fractional pathloss-inversion power control policy is used for the uplink in [34]. For the case of equal spectral resources to each UE connected to a base station, this policy is identical to a path-loss inversion power control policy. In Chapter 5, it is shown that with such a policy, biasing for the uplink does not produce large gains over uplink pathloss association, which itself

produces a small but consistent gain over coupled association with optimal biasing for the downlink.

These gains are further affected by the use of dual or multi-slope path loss models, which punish large distances much more heavily than they punish small distances. Most of the work described above uses fixed, identical, single slope path loss models for all tiers. In this work, it is shown that the gain is smaller for higher path loss exponents.

Chapter 3

System Model

This work uses stochastic geometric modeling techniques introduced in [6], where both base stations and users are drawn from a Poisson Point Process. Figure 3.1 shows voronoi tessellations for both single-tier networks (under grid and PPP models) and two-tier networks with a transmit power differential, and Figure 3.2 shows networks at various densities. This thesis is simulation-based and so does not immediately realize tractability benefits associated with stochastic geometric models. However, the thesis does benefit from the accuracy of stochastic geometric models: PPPs have been shown to more closely model real-world realizations of networks than grid models and provide a lower bound for most capacity and probability of coverage results [6, 36]. Furthermore, recent work has shown that a constant "deployment gain" can be used to easily convert the coverage distribution (with respect to a threshold) from a PPP model to the distribution of a deployment [37]. Future work will use insights from simulation to derive analytic results.

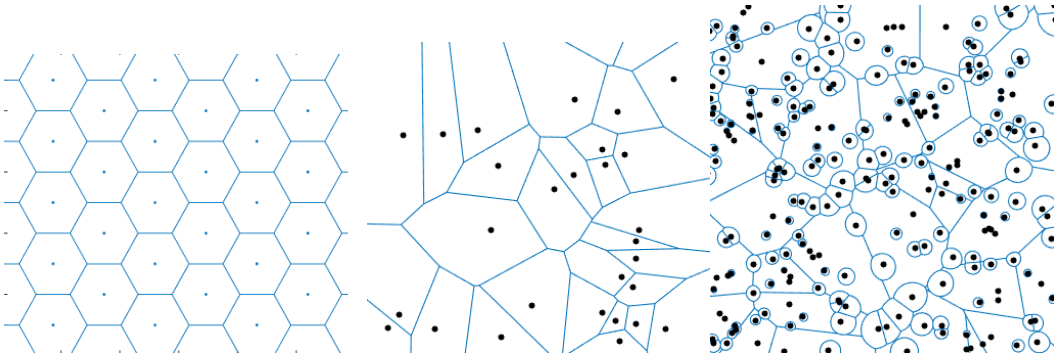

(a) (b) (c)

Figure 3.1: Voronoi tesselations for a standard grid model, a single-tier network, and a two-tier network with 13 dB transmit power difference, respectively.

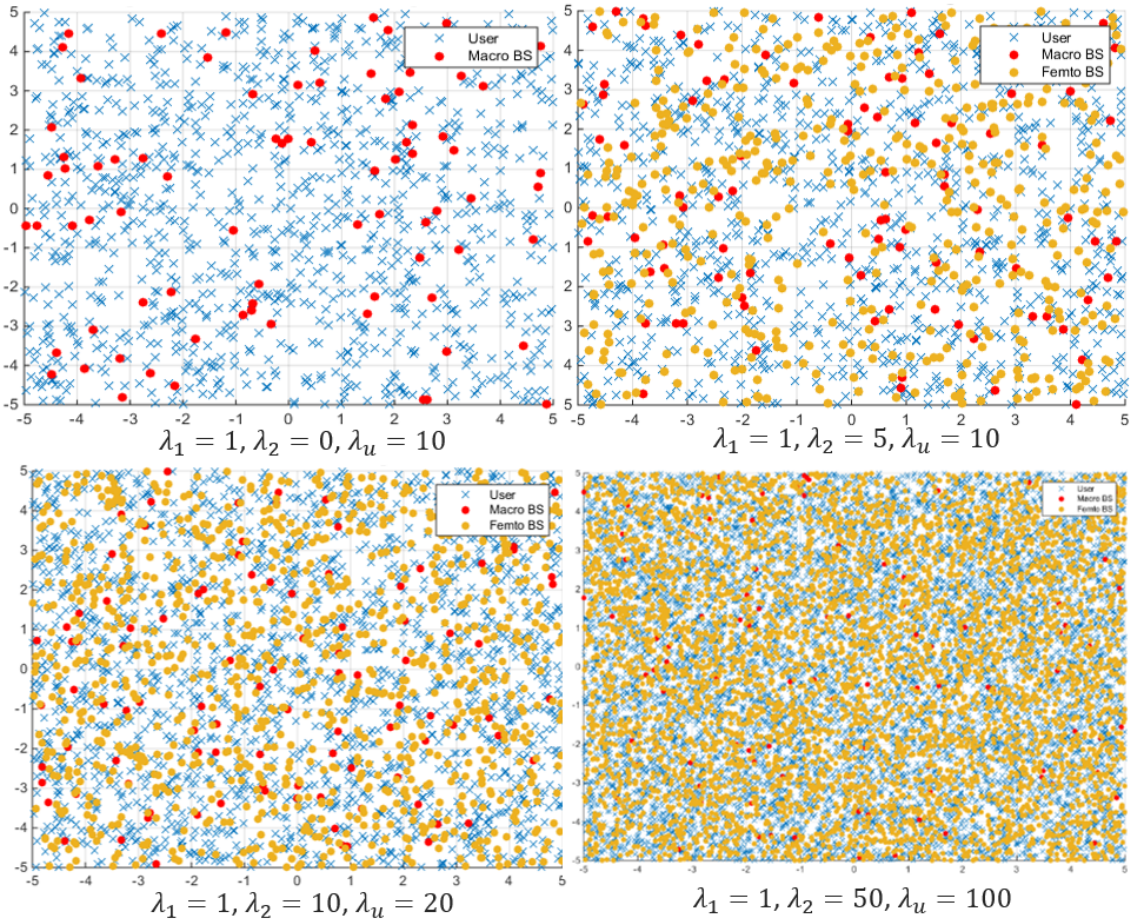

Figure 3.2: Two-tier networks with various densities.

UEs and BSs in each tier i are placed using Poison Point Processes (PPPs) with densities λ_u and λ_i, respectively. A sample p is drawn from a Poisson distribution with mean λ, and p points from a 2-D uniform distribution are drawn on the grid $[-g, g]$. Users are associated with base stations, and base station load (for the BS to which the user at the origin is connected), SINR, $\mathrm{P}_{\mathrm{coverage}}$, and rate are calculated for the user at the origin. These values are measured over many experiments to generate distributions given each set of parameters.

Without loss of generality, all measurements are made with respect to a fixed user at the origin. A full list of parameters is included in Table 3.1 on page 35.

3.1 Signal Propagation Model

This work uses a propagation model similar to those in [6] and [7]. This section details each component of the model.

3.1.1 Channel Model

A Rayleigh Fading channel model is assumed by default. A channel value h_{k,i_j} between user k and base station j in tier i is drawn from iid exponential distributions $p_x(h_{k,i_j}, \lambda) = \lambda e^{-\lambda x}$, where $\lambda = 1$.

3.1.2 Path Loss Models

A contribution of this thesis is to illustrate how the use of dual-slope path loss models affects design choices. Following [7], the single-slope and dual-slope path loss equations are given in (3.1) and (3.2), respectively:

$$P_r = h_{k,i_j} P_t K |\frac{x}{d_0}|^{-\alpha} \tag{3.1}$$

where K encapsulates all system parameters.

$$P_r = \begin{cases} h_{k,i_j} P_t K |\frac{x}{d_0}|^{-\alpha_0} & x \leq R_c \\ R_c^{\alpha_1 - \alpha_0} h_{k,i_j} P_t K |\frac{x}{d_0}|^{-\alpha_1} & x > R_c \end{cases} \tag{3.2}$$

where the $R_c^{\alpha_1 - \alpha_0}$ factor is used for continuity purposes. Figure 3.3 shows received power (without fading) depending on different path loss exponents, with $R_c = 200$m and $d_0 = 100$m.

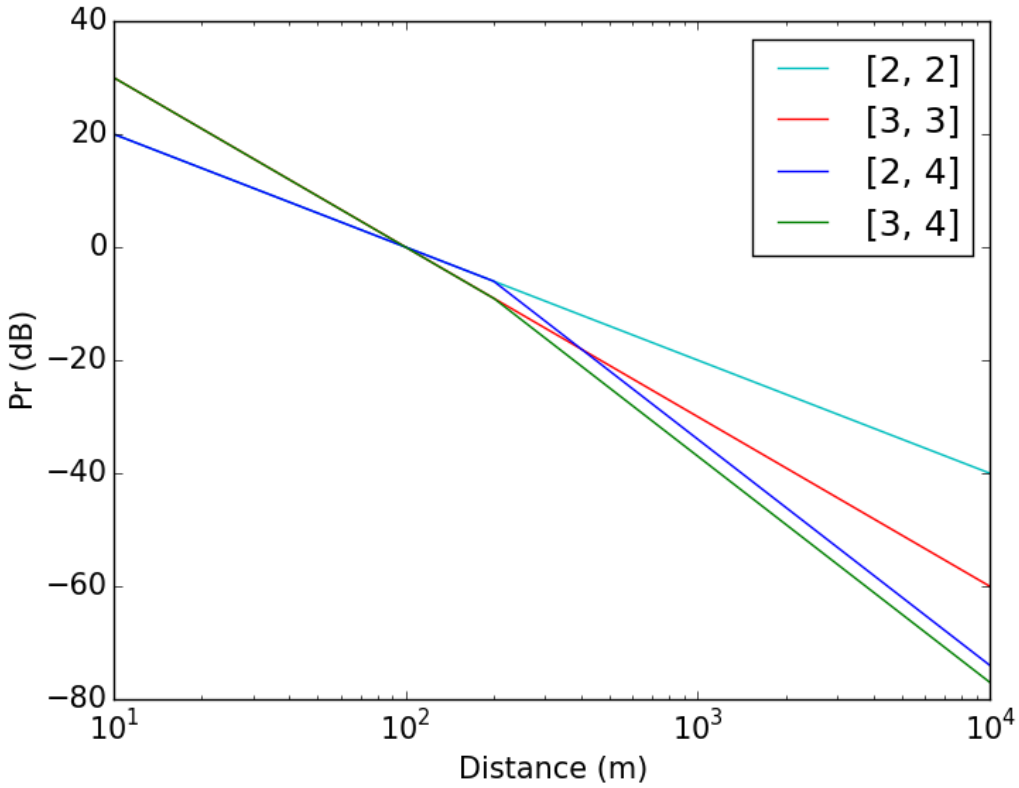

Figure 3.3: P_r based on distance, without fading, from a base station with $P_t = 0$ dBW

3.1.3 Uplink Power Control

Truncated channel inversion is used in the uplink. Figure 3.4 shows the uplink power as a function of distance from the BS (on average with fading).

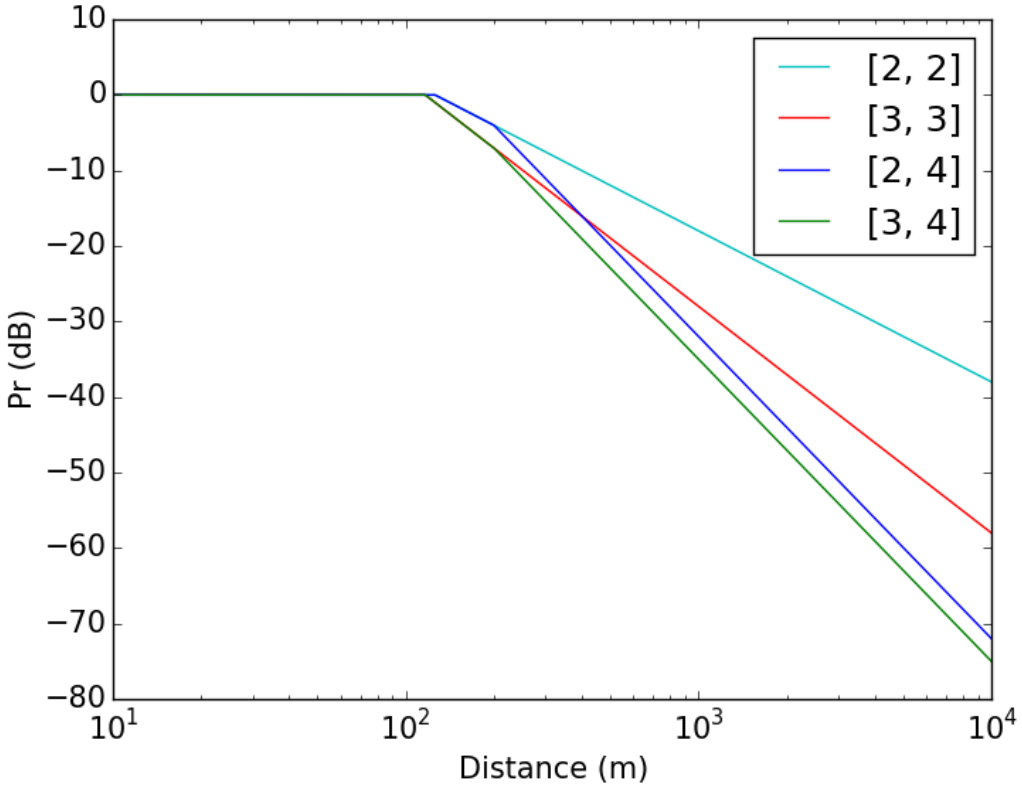

Figure 3.4: Truncated channel inversion for the uplink

3.2 Downlink Association

For downlink association, two standard techniques are analyzed: highest received SNR, and SNR with biasing. Future work can extend these simulations by integrating load balancing user association.

3.2.1 Highest Received SNR

A user k is associated with the base station j in tier i that maximizes

$$\arg\max_{i_j}(\gamma(dB) = P_{r,i_j} - \sigma^2) \tag{3.3}$$

where all terms are in dB. Note that such an association differs from association in real networks, where a UE can easily determine SINR from each base station using reference signals. In large simulations with thousands of base stations and users, interference cannot be taken into account when associating each user because the run-time of the code would scale by $O(N_{\text{Users}} \times N_{\text{base stations}})$, which is not tractable. SNR association is also used in [32] and [33], which similarly use simulations. This limitation does not largely affect results because interference affects rate both linearly (through proportional allocation) and inside the log function, and only the term inside the log function would differ if SINR association is used.

3.2.2 Biasing

A user k is associated with the base station j in tier i that maximizes

$$\arg\max_{i_j}(\gamma(dB)_{biased} = P_{r,i_j} + B_i - \sigma^2) \tag{3.4}$$

where all terms are in dB. Optimal biases are found for various λ_i pairs.

3.3 Uplink Association

Two strategies are also used for uplink association: coupled with the downlink (both with and without biasing), and decoupled with highest received SNR.

3.3.1 Coupled Association

For the base measurements, uplink is coupled with downlink, and so a user k is associated with the base station j in tier i that maximizes either received power or receive power with bias.

3.3.2 Highest Received SNR at the base station

A user k is associated with the base station j in tier i that maximizes uplink received power.

$$\arg\max_{i_k}(\gamma_{uplink}(dB) = P_{r,uplink} - \sigma^2) \tag{3.5}$$

$$P_{r,uplink} = \begin{cases} h_{k,i_j} + K + P_{t,u} - 10\alpha_0 \log_{10} |\frac{x}{d_0}| & x \leq R_c \\ h_{k,i_j} + K + P_{t,u} - 10R_c^{\alpha_1-\alpha_0}\alpha_0 \log_{10} |\frac{x}{d_0}| & x > R_c \end{cases} \tag{3.6}$$

where all terms are in dB, and $P_{t,u}$ integrates truncated channel inversion. Note that $P_{r,uplink}$ does not depend on the base station to which the user is connected. Thus, this association rule is the same as transmitting to the BS that receives the highest SNR from the user (with fading). Equations 3.7 and 3.8 give the exact uplink association rules for single and dual-slope path loss models, respectively.

$$\arg\max_{i_j} h_{k,i_j} K |\frac{x}{d_0}|^{-\alpha} \tag{3.7}$$

$$\arg\max_{i_j} \begin{cases} h_{k,i_j} K |\frac{x}{d_0}|^{-\alpha_0} & x \leq R_c \\ R_c^{\alpha_1-\alpha_0} h_{k,i_j} K |\frac{x}{d_0}|^{-\alpha_1} & x > R_c \end{cases} \tag{3.8}$$

3.4 Measurements

Thousands of simulations are run for each parameter combination. Several measurements are calculated for each experiment and then aggregated at for each parameter combination. For each experiment, relevant calculations are for the user at the origin.

3.4.1 SINR

Using the above models, the final received power and SINR from base station j in tier i are shown in (3.9) and (3.10). Note that in-cell interference is assumed to be perfectly nulled.

$$P_{r,i_j} = h_{i_j} P_{t,i} \tag{3.9}$$

$$\gamma_{downlink} = \frac{P_{r,i_j}}{\sum_{l \neq j} P_{r,i_l} + \sigma^2} \tag{3.10}$$

3.4.2 Rate

Full Channel State Information at the Transmitter (CSIT) is assumed with rate modulation. A user receives a rate r from base station j in tier i when SINR $\geq T$, as shown in Equation 3.11.

$$r = \begin{cases} \frac{W_i}{\mathrm{l}_{i_j}} \log_2(1+\gamma) & \gamma \geq T \\ 0 & \gamma < T \end{cases} \tag{3.11}$$

This rate calculation translates to a system with fair, orthogonal resource partitioning.

3.4.3 Probability of Coverage

Given a SINR threshold T,

$$\begin{aligned} \mathrm{P}_{\mathrm{Coverage}} &= \mathbb{E}\left[\mathbb{1}_{\gamma > T}\right] \\ &= \frac{\text{Number of Times}(\gamma > T)}{\mathrm{N}_{\mathrm{experiments}}} \end{aligned}$$

3.4.4 Optimal Bias

For several of the experiment setups, an optimal bias is found for each set of parameter combinations. For example, an optimal bias is found for different relative densities between the tiers and for transmit power differentials. The optimal bias is the bias that maximizes the log sum rate, as shown in (3.12).

$$B_{optimal} = \arg\max_{B_1} \sum_{\text{experiments}} \log\, r \tag{3.12}$$

Chapter 4

Methods

4.1 Simulation Setup

An extensible network simulator in C++ for large-scale, efficient simulations of multi-tiered networks was developed as part of this thesis. For each experiment described in Chapter 5, 3000 simulations are run with the model described in Chapter 3. For each simulation, base station and user locations and counts are determined as a realization of their respective PPPs.

A key benefit of the simulation software is the ability to plug in different configurations and run them with minimal code overhead. The various user association techniques described in Section 3.2 are used consecutively in experiments, and their results compared. Arbitrary path loss models are plugged into the system, and simulations are used to generate results comparing single-slope and multi-slope path loss models.

Furthermore, this simulation setup can be used to simulate and compare a wide variety of parameter combinations. Any levels of heterogeneous network tiers can be simulated, with each tier following its path loss model, transmission power, and base station association characteristics. Performance can be evaluated at high density regimes, along with settings with differential density and power at each base

station.

The data generated by each experiment is stored in Comma Separated Value (CSV) files to be post-processed. Each experiment is summarized with parameter values and the key performance metrics discussed in Section 3.4. Python is then used to parse the CSV files and create plots.

4.2 Performance Benchmarks

Figure 4.1 compares performance for C++ and Matlab to complete identical tasks. The run-time of the simulator is largely determined by the time it takes to associate users to base stations – naively, the distance between each user and each base station must be found so that the signal strength can be calculated. This task can be done efficiently using a k-nearest neighbor algorithm. However, the limitation does prevent taking into account interference in association. The performance metrics in the figure were obtained by running k-nearest neighbors and a full simulation on Matlab and C++ . The programs were run on different machines: the Matlab code was run on a quad-core i7 machine running Windows, and the C++ code was run on a dual-core Ubuntu virtual machine running on that Windows box. Normalized to similar CPU performance specifications, the C++ code is approximately 20 times faster than the Matlab code. This gain is not drastic for small simulations. However, for simulations that take multiple days such as those in this thesis, the gain is essential. Furthermore, C++ can easily be parallelized and run on multiple cores with minimal effort.

4.3 Simulator Verification

The code and model was first verified by comparing its output to analytic results derived in [7]. A single-tier network with $[\alpha_0, \alpha_1] = [2, 4]$ and $[3, 4]$ was simulated. Table 4.1 details all parameters used in the experiment.

Figures 4.2, 4.4, 4.3, 4.5, 4.6 compare the output of the simulation code in this thesis to images from [7]. The simulation curves match well with both analytic and simulation results from literature, indicating that the simulator is well-suited to analyze new configurations and questions. Furthermore, the images indicate the key result from the literature: in a single-tier network using dual-slope path loss models, there is a state transition at $\alpha_0 = 2$ in the probability of coverage and SIR with asymptotic density.

Symbol	Description	Value or Range (if applicable)
N_{tiers}	Number of tiers.	2
λ_u	User density. λ_u users per square kilometer.	200 UEs/km^2
λ_i	Base station density for tier i. λ_i base stations per square kilometer.	.1 BS/km^2 to 1000 BS/km^2
W_i	Bandwidth available at tier i.	1×10^6 Hz
$[-g, g]$	Grid limits in each X and Y directions.	$[-10, 10]$
h_{jk}	Channel between user k and base station j.	iid exponential RV with $\mu = 1$
$P_{t,i}$	Power transmitted by each base station in tier i.	13 dBW for Macro, 0 dBW for Femto
σ^2	Noise Power	-10 dBW
$[\alpha_0, \alpha_1]$	Path Loss Exponents	$[2, 2], [2, 4], [3, 3]$, and $[3, 4]$
d_0	Reference distance	100 m
R_c	For dual-slope path loss models, the critical distance at which to use α_1. The value used in this work is bigger than typical, but results will qualitatively remain the same with a smaller value.	200 m
T	Minimum SINR below which an outage is declared.	-10 dB
B_i	Bias in user association for each base station in tier i.	0 dB to 20 dB
P_r	Power received by the user at the origin.	
γ	Signal to Interference and Noise Ratio	
P_{Coverage}	Probability of Coverage for user at the origin with threshold T.	
Rate	Supported rate for user at origin.	

Table 3.1: Simulation parameters and measurements. Note: Each base station within a tier is considered to be in-band. To model systems in which k independent channels are available to each tier, k tiers each with base station density of λ_i/k and power P_i/k can be used. Assuming the bands are independent, power is equally divided between the channels and there is no inter-band interference.

Table 4.1: Parameters for model verification

Parameter	**Value**
N_{tiers}	1
λ_u	50 UEs/km^2
λ_0	.01 BS/km^2 to 315 BS/km^2
W_i	1 Hz
$P_{t,i}$	0 dB for all BSs
σ^2	$-\infty$ dB and 0 dB
$[\alpha_0, \alpha_1]$	$[2, 4]$ and $[3, 4]$

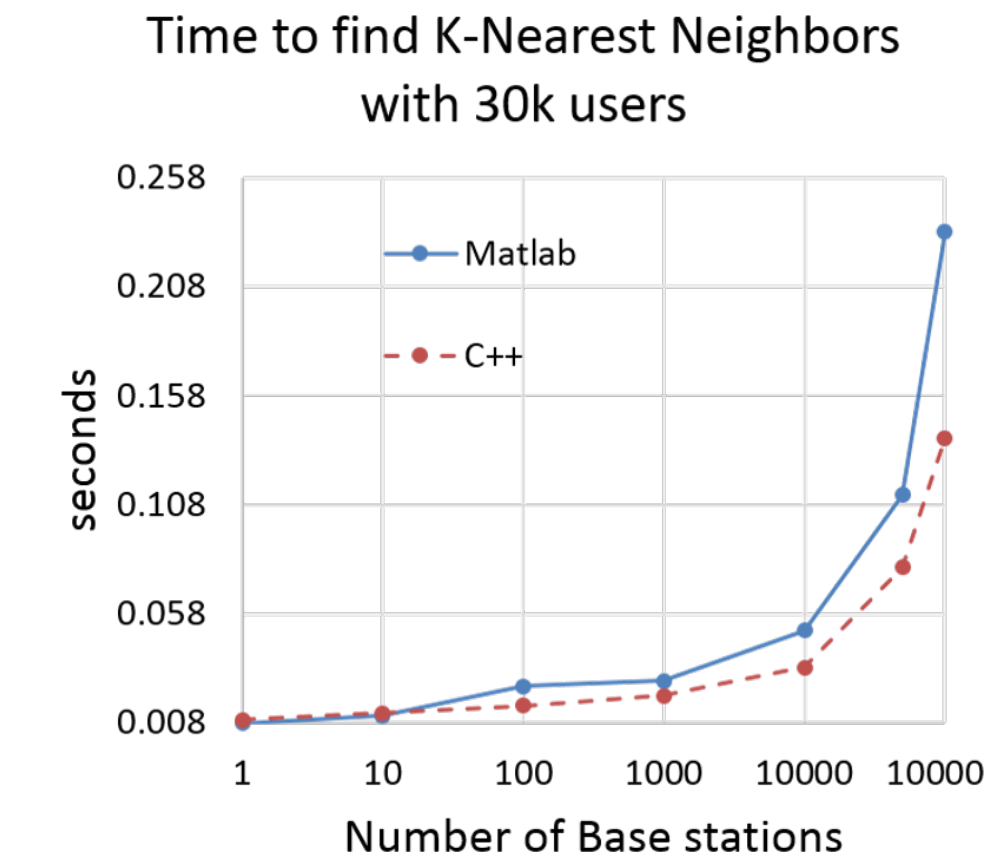

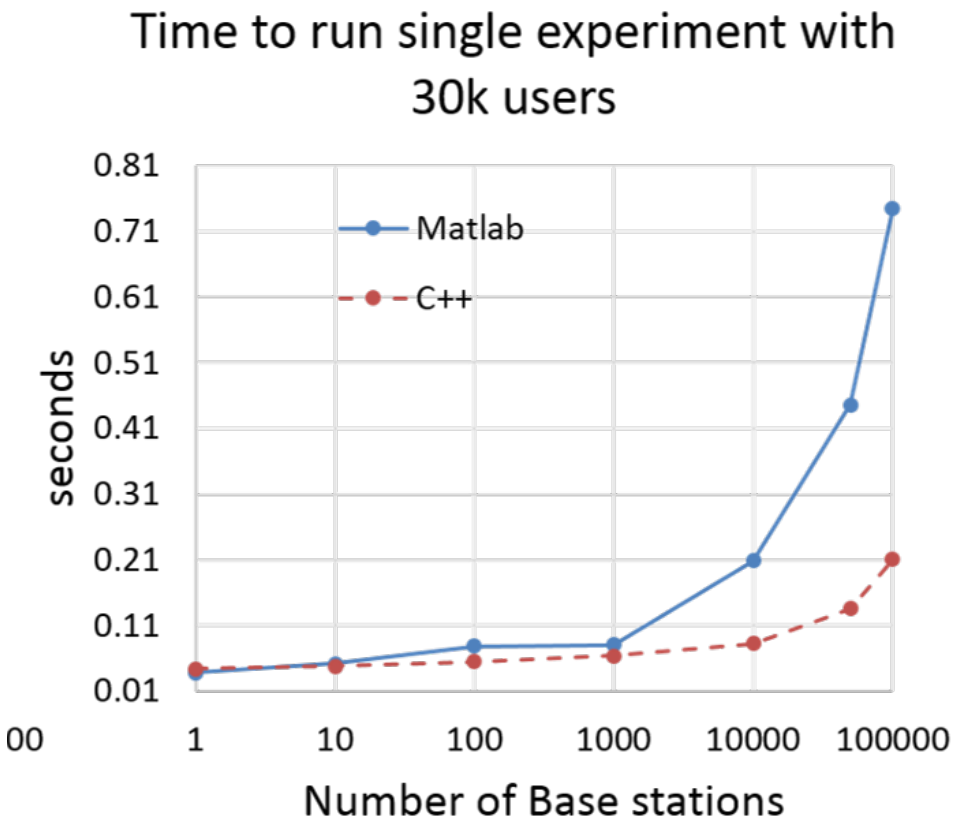

Figure 4.1: Performance of Matlab and C++ code.

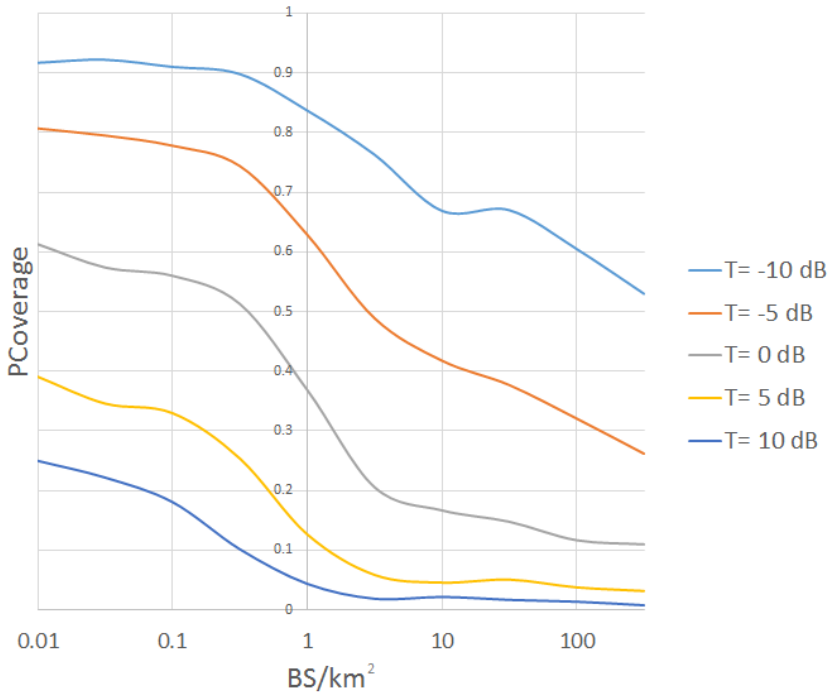

(a) Simulation results for SIR with $\alpha_0 = 2, \alpha_1 = 4$ from this work's simulator

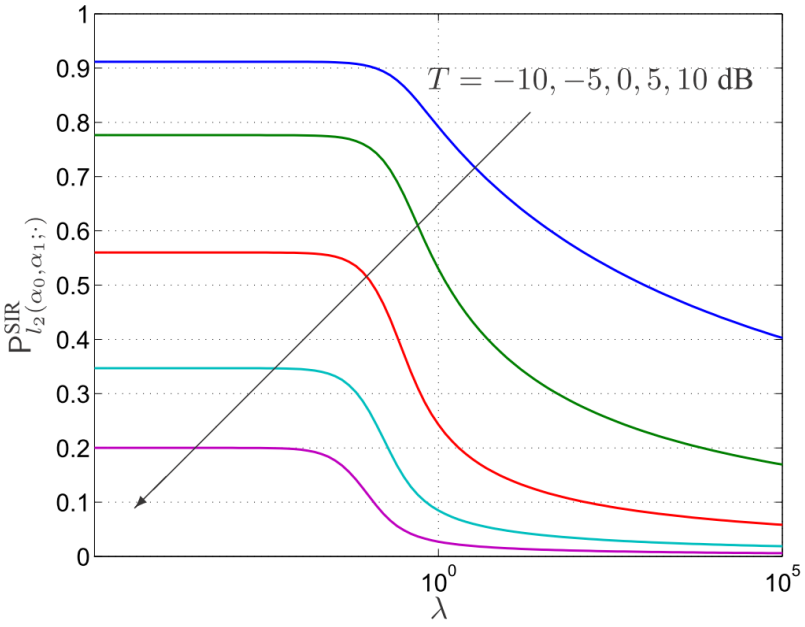

(b) Image from [7]. Analytic results for SIR with $\alpha_0 = 2, \alpha_1 = 4$

Figure 4.2: Verification SIR for a single-tier network with $\alpha_0 = 2, \alpha_1 = 4$ from analysis and simulation. Note that the simulation results match almost perfectly with analytic results for the simulated density range.

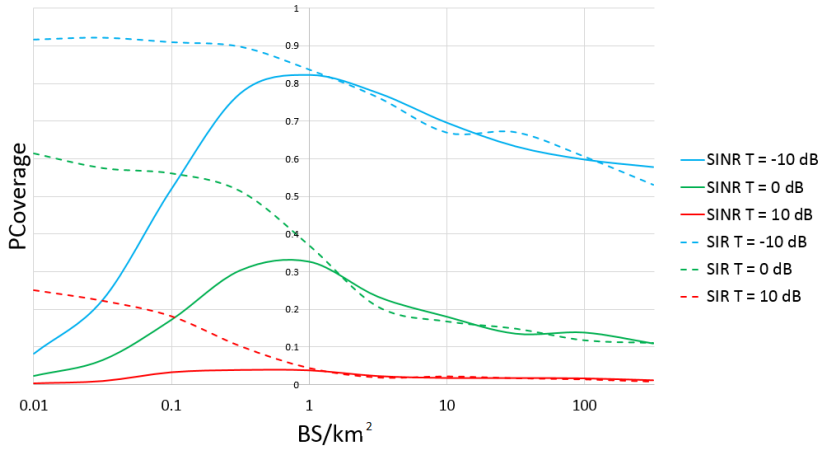

(a) Simulation results for SIR and SINR with $\alpha_0 = 2, \alpha_1 = 4$ from this work's simulator

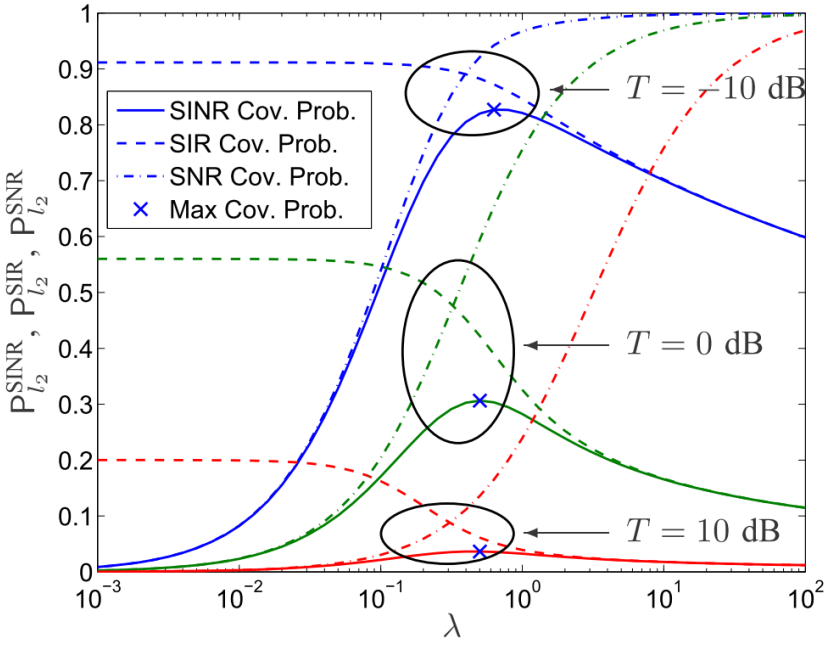

(b) Image from [7]. Analytic results for SIR with $\alpha_0 = 2, \alpha_1 = 4$

Figure 4.3: Verification SIR and SINR for a single-tier network with $\alpha_0 = 2, \alpha_1 = 4$ from analysis and simulation. Note that the simulation results match almost perfectly with analytic results for the simulated density range.

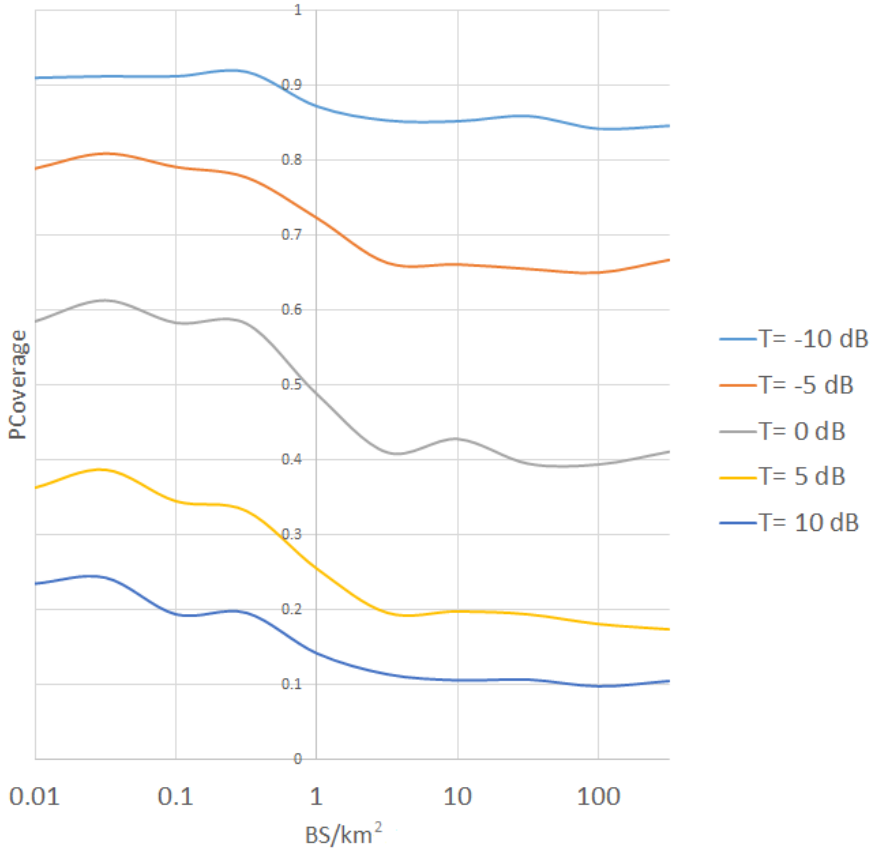

(a) Simulation results for SIR with $\alpha_0 = 3, \alpha_1 = 4$ from this work's simulator

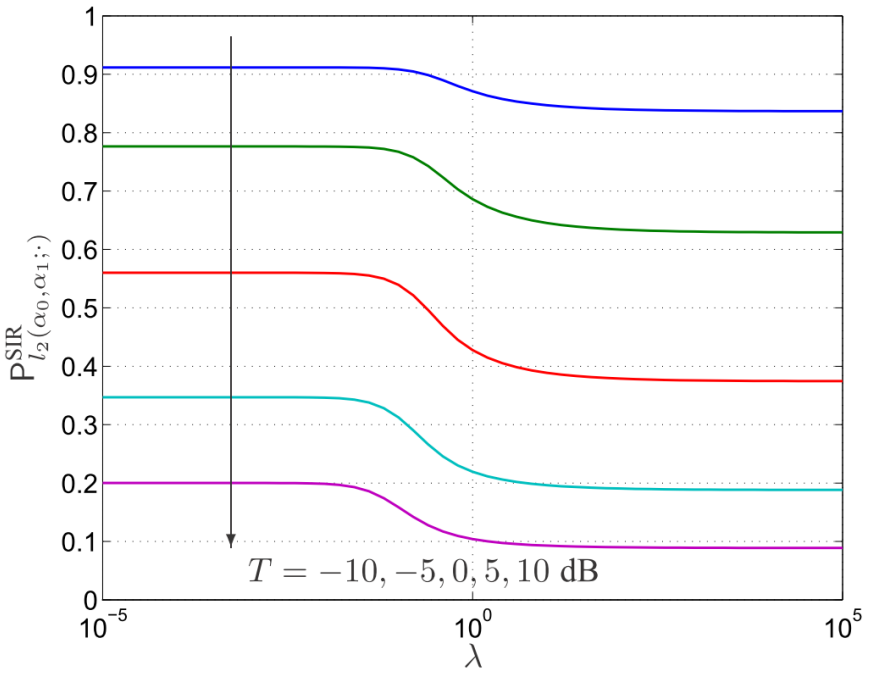

(b) Image from [7]. Analytic results for SIR with $\alpha_0 = 3, \alpha_1 = 4$

Figure 4.4: Verification SIR for a single-tier network with $\alpha_0 = 3, \alpha_1 = 4$ from analysis and simulation. Note that the simulation results match almost perfectly with analytic results for the simulated density range.

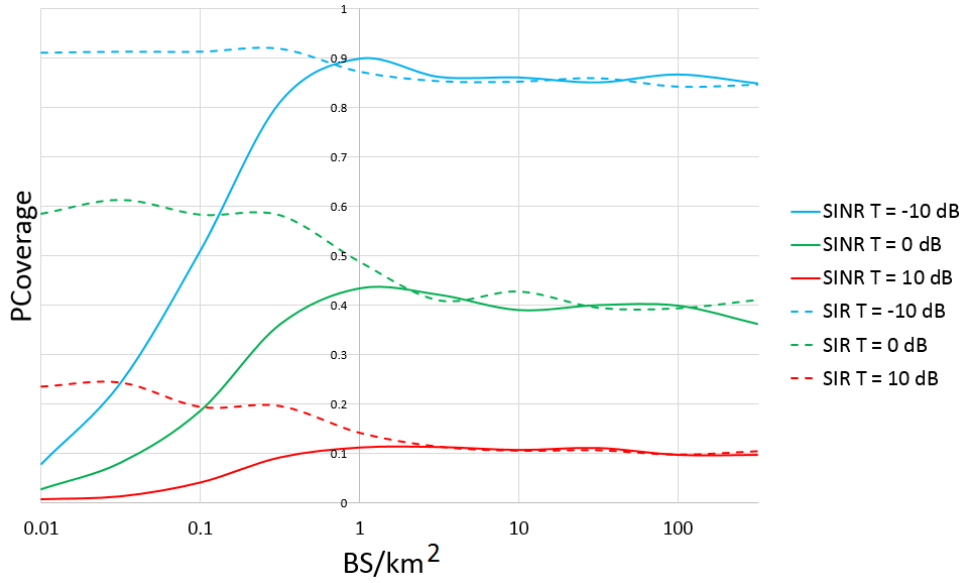

(a) Simulation results for SIR and SINR with $\alpha_0 = 3, \alpha_1 = 4$ from this work's simulator

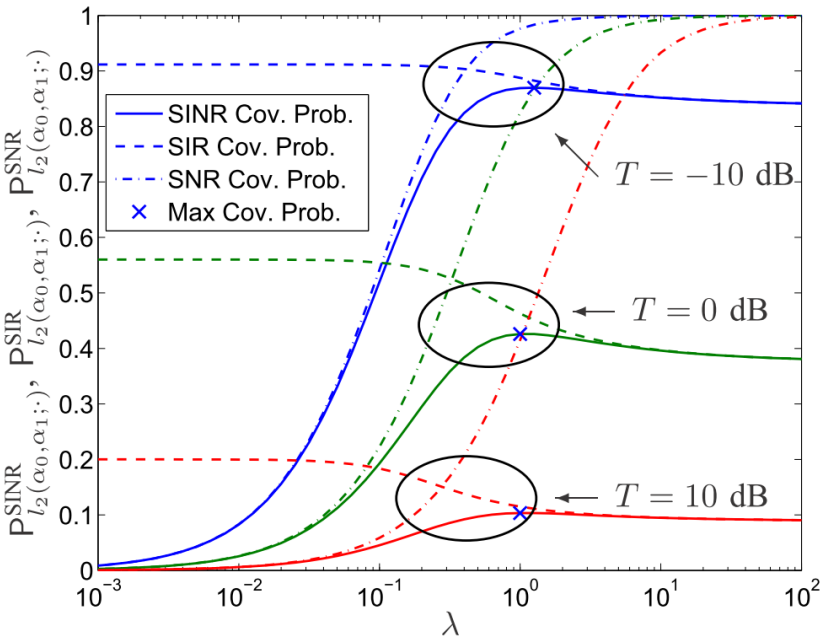

(b) Image from [7]. Analytic results for SIR with $\alpha_0 = 3, \alpha_1 = 4$

Figure 4.5: Verification SIR and SINR for a single-tier network with $\alpha_0 = 3, \alpha_1 = 4$ from analysis and simulation. Note that the simulation results match almost perfectly with analytic results for the simulated density range.

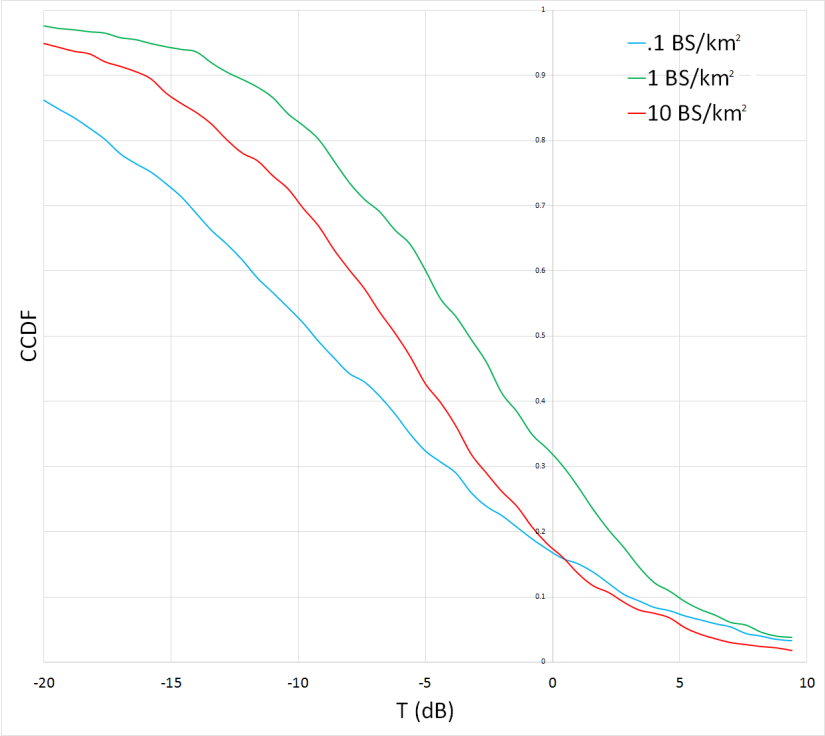

(a) Simulation results for SINR CCDF with $\alpha_0 = 2, \alpha_1 = 4$ from this work's simulator

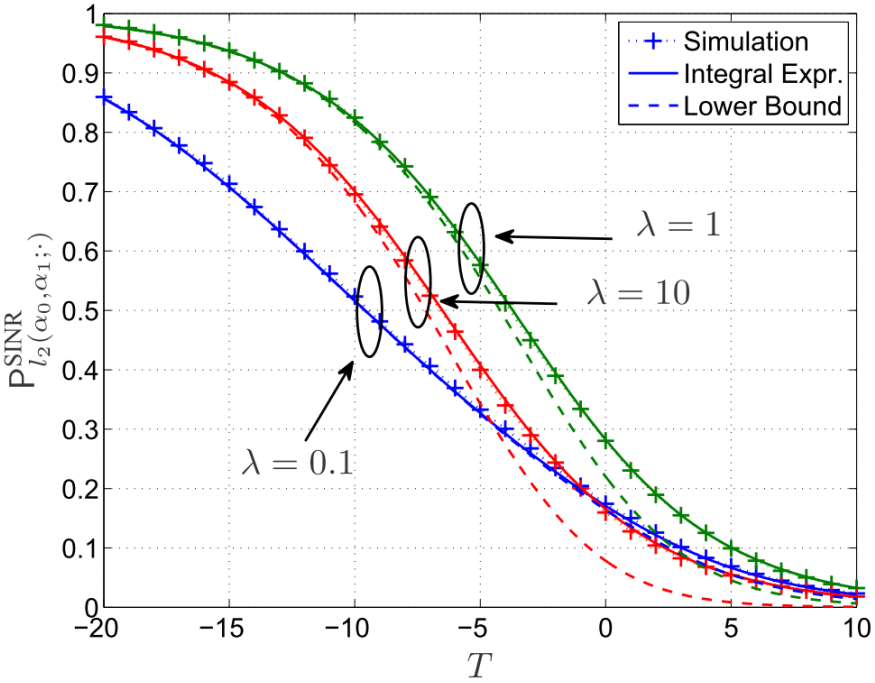

(b) Image from [7]. Analytic and simulation results for SINR CCDF with $\alpha_0 = 2, \alpha_1 = 4$

Figure 4.6: Verification SINR CCDF for a single-tier network with $\alpha_0 = 2, \alpha_1 = 4$ from analysis and simulation. Note that the simulation results match almost perfectly with analytic results for the simulated density range.

4.4 Discussion

This simulation methodology counters recent academic research trends in two ways. First, complex software simulations of this variety are generally not used for academic research. The main criticism for this approach is that such simulations are only useful in producing insight for analysis later. Furthermore, such simulations often produce noisy results and take a long time to run, especially if numerous parameter combinations are studied. However, an initial simulation approach is necessary for insights when numerous parameter values and strategies interact.

Second, this thesis simulated networks using C++ , rather than Matlab, which is preferred in academic circles. As discussed in Section 4.2, the C++ simulations are about 20 times faster when normalized to the same machine parameters. This speed-up is important when optimizing a large number of parameters together as it allows many parameter combinations to be simulated. Using C++ is essential for the results in this work.

Chapter 5

Experiments and Results

Two classes of problems were analyzed in this work. First, experiments were run regarding the benefits of static biasing with different path loss models. Then, uplink/downlink decoupling was analyzed for different path loss models and downlink user association techniques.

5.1 Optimal Static Biasing

Optimal biasing was analyzed for two cases: when the density differential between the tiers increases asymptotically, and when the density of each tier increases together.

5.1.1 Relative Density Disparity

In this experiment, the density of the small cell tier was increased while the density of the macro tier was held constant at 1 BS/km^2. As the small cell density increased, the log sum rate and other metrics were calculated for each bias value between 0 and 20 dB. Table 5.1 contains the full parameters for this experiment.

Results. Along with log sum rate, the simulation tracked the tier to which the UE at the origin connected as the density of the small cells increased. Figure 5.1

Parameter	Value
λ_0	1 BS/km^2
λ_1	.3 BS/km^2 to 315 BS/km^2
B_0	0 dB
B_1	0 dB to 20 dB

Table 5.1: Parameters for optimal biasing with density of femto tier increasing. All parameters not included are the same as in Table 3.1

shows the fraction of users which connected to the small cell tier for different path loss models and densities, without any biasing and with a 20 dB bias. One surprising result is that biasing flips the effect the path loss model has on predicting to which tier the UE will connect. Without biasing, as the path loss exponents increase, more UEs connect to small cells because they are closer. However, with biasing, the greater the path loss the more likely a UE is to connect to a macro tier. This result can be explained as follows: the variance of SNR values is smaller for lower path loss values (far away base stations have higher SNRs), and so a given static bias affects systems with lower path loss exponents more.

Furthermore, the path loss model used has a large effect on biasing gain. Figure 5.2 shows the log sum rate with and without optimal biasing (the bias that maximizes the log sum rate). Figure 5.3 shows the gain from biasing for the different path loss models as density increases. Note that, the larger the path loss exponents, the less useful biasing is. This result can be seen as a direct effect of the previous result: the smaller the path loss exponent, the more UEs are associated with small cells. The macro cells thus become less loaded, and each UE can receive more resources. Similarly, when the femto tier has a much larger density than the macro

tier, as would happen in a realistic realization, biasing gains disappear. These results suggest the importance of carefully choosing path loss exponents and density when analyzing the gains of various user association models. A user association strategy may not yield predicted gains if a network realization has different parameters than used in the analysis.

Next, it is instructive to note how the optimal bias values themselves change with relative density. Figures 5.4 and 5.5 show the optimal bias values that maximize the log sum rate and probability of coverage, respectively. Even with large averaging and iterative runs that attempt to converge on an optimal value, the optimal values are noisy. However, there is a clear negative relationship between density differential and optimal biasing on each graph. This thesis posits that the trend is due to the following tradeoff: at low differential density, most users receive a higher SNR from the macro cell, which can thus provide fewer resources to each user. As the density increases, however, there base station load is not a concern, and biasing away from a stronger macro cell is harmful. These results do not extend to the case where the density of each tier varies jointly, as is discussed in the next section.

Finally, as expected, biasing does not change the trends in probability of coverage for different path loss models, as derived in [7]. Figure 5.6 shows that, though optimal biasing for probability of coverage may produce gains at a low density differential, the asymptotic trends with relative density remain the same. There is a phase transition at $\alpha_0 = 2$ where probability of coverage tends to zero as density increases. Note that the gain observed is a direct effect of the SNR association rule. With SINR association, there would be no gain in probability of coverage with

biasing – biasing would strictly reduce probability of coverage. As such, this gain would not occur in real systems.

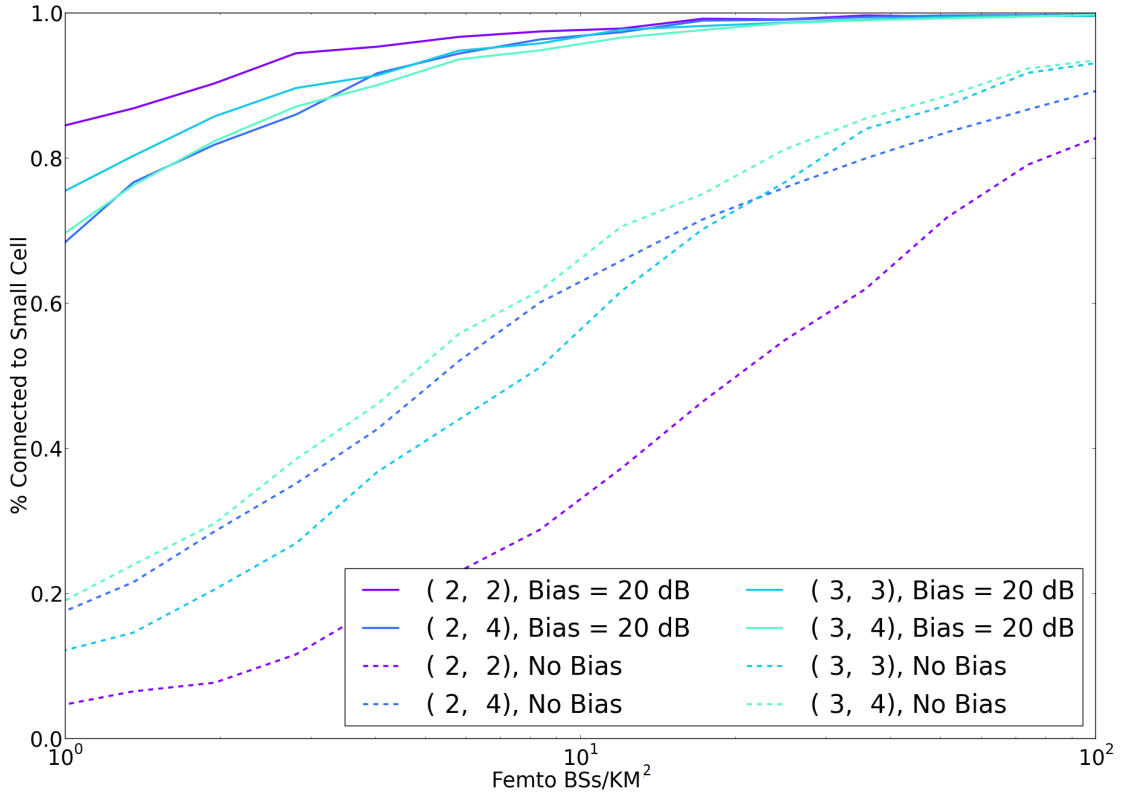

Figure 5.1: Fraction of UEs that connect to small cells as the density differential increases

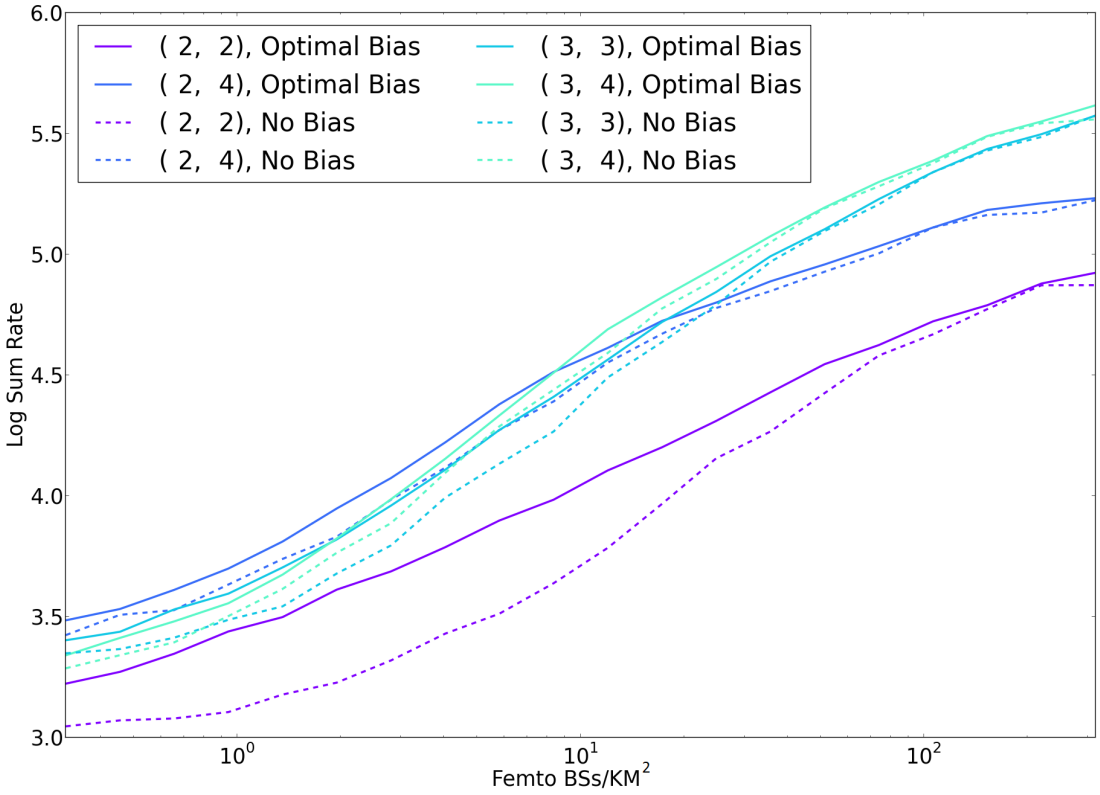

Figure 5.2: Log sum rate with and without biasing as relative density increases

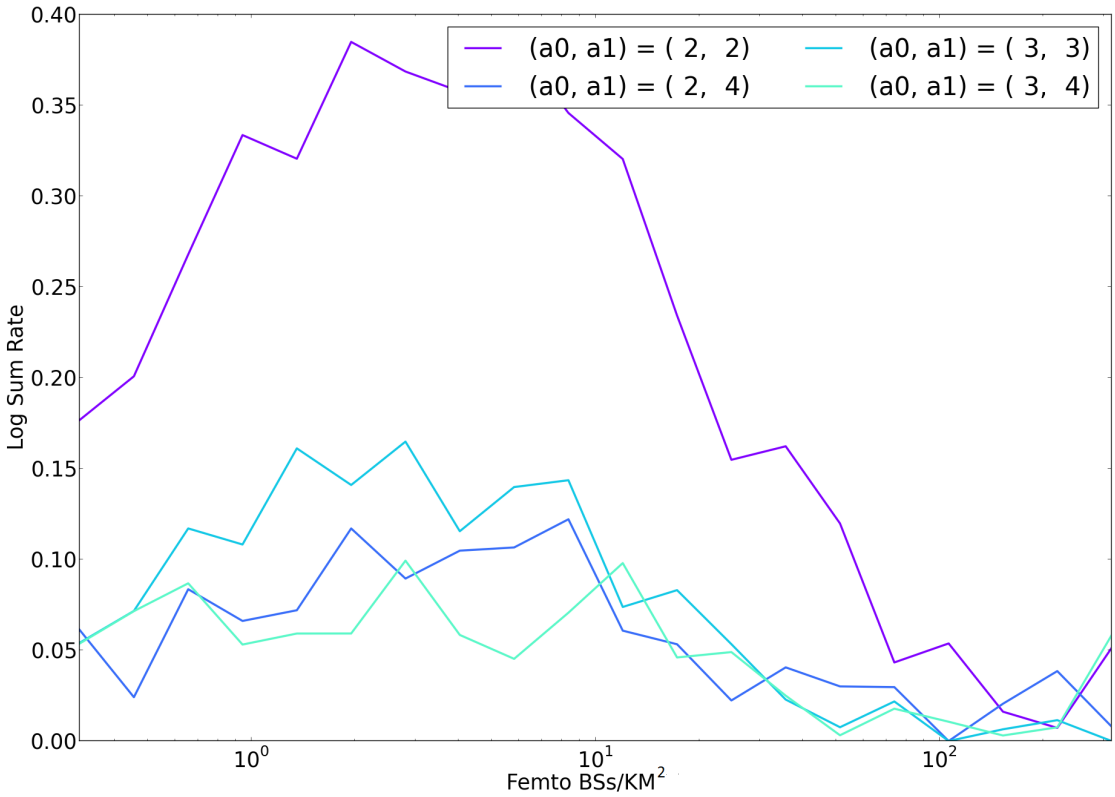

Figure 5.3: Gain in log sum rate from biasing as relative density increases

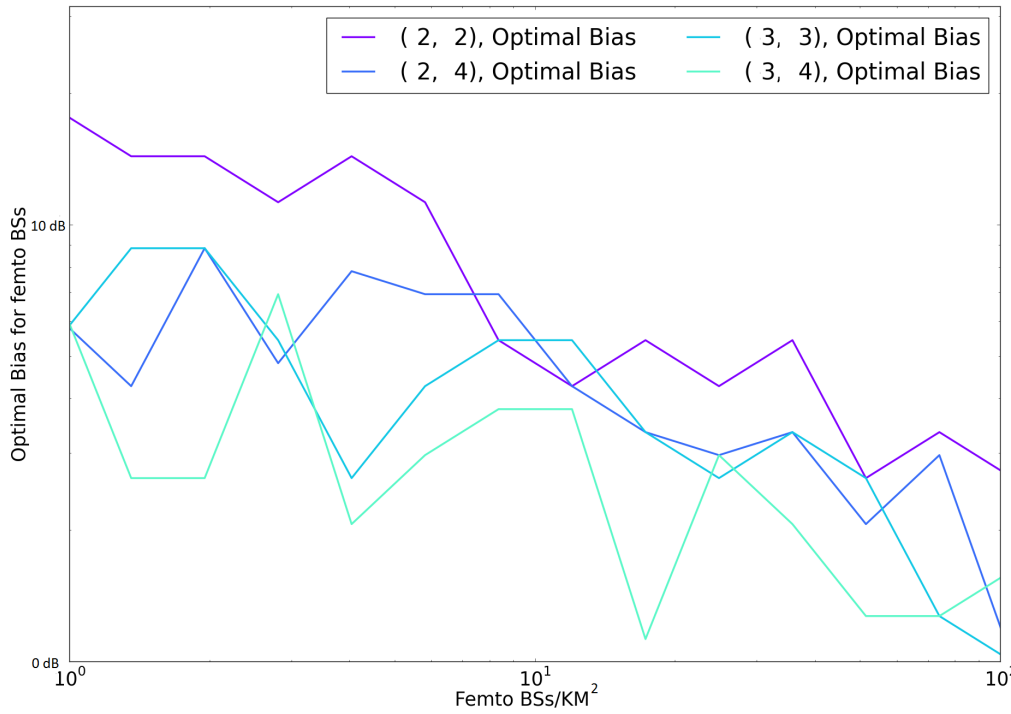

Figure 5.4: Optimal bias that maximizes the log sum rate as density differential increases.

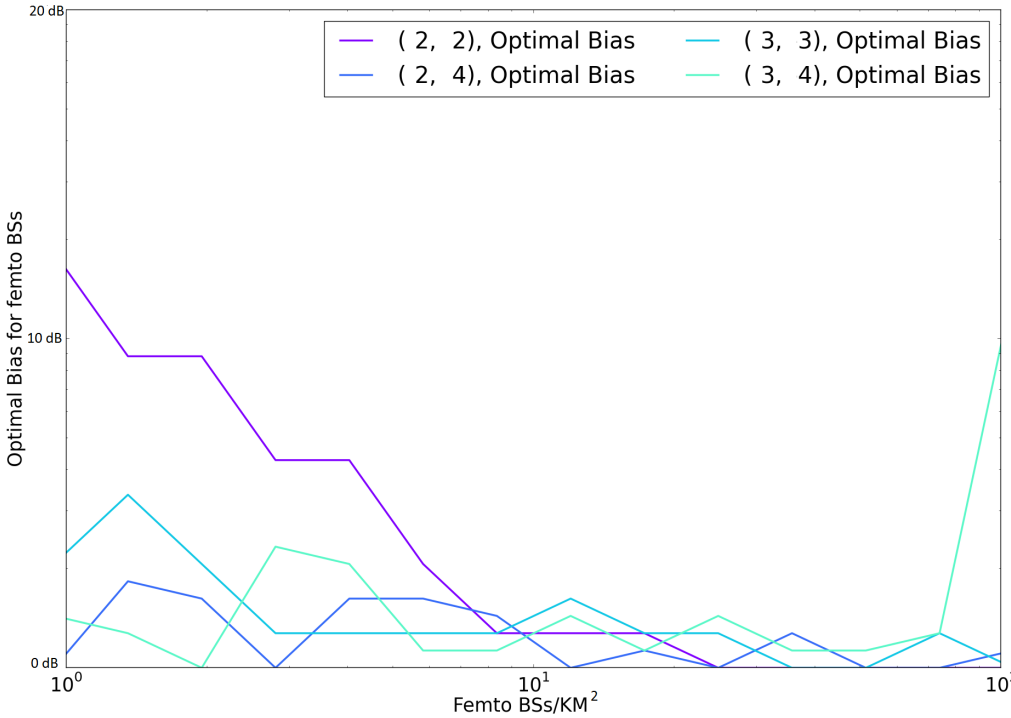

Figure 5.5: Optimal bias that maximizes probability of coverage as density differential increases.

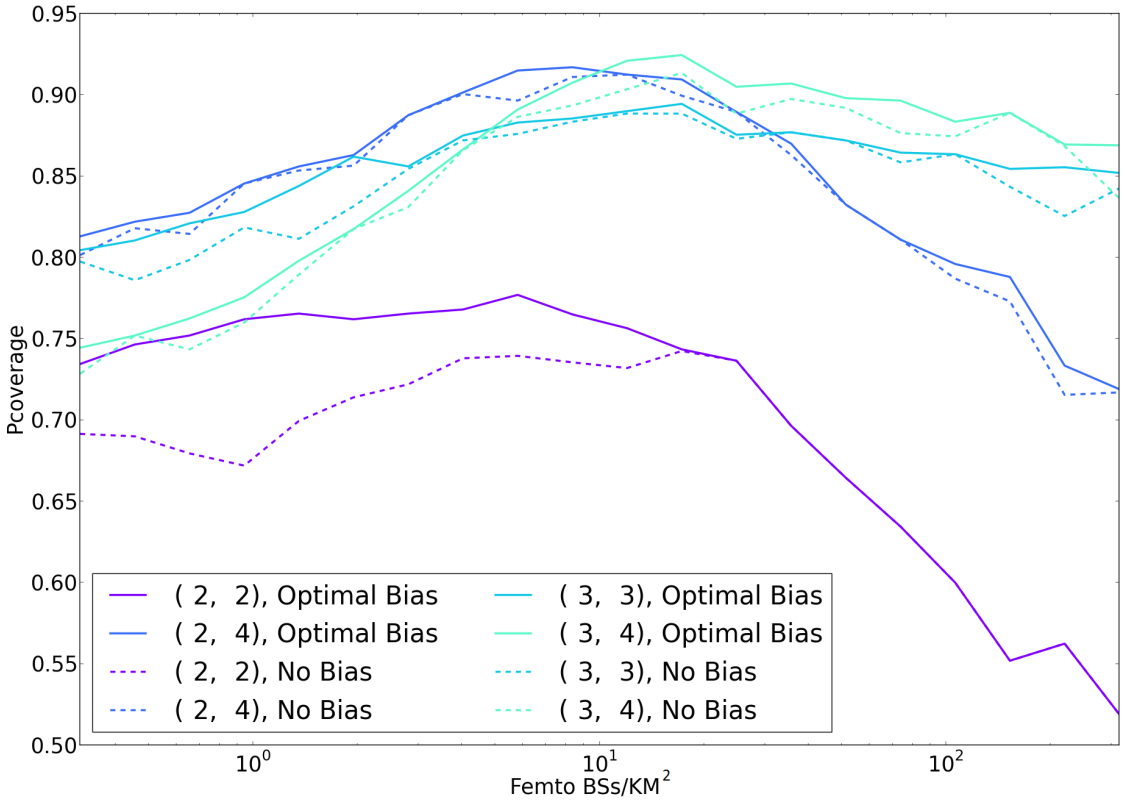

Figure 5.6: Probability of coverage with optimal biasing as relative density increases.

Parameter	Value
λ_0	.3 BS/km^2 to 315 BS/km^2
λ_1	.3 BS/km^2 to 315 BS/km^2
B_0	0 dB
B_1	0 dB to 20 dB

Table 5.2: Parameters for optimal biasing with density of each tier increasing. All parameters not included are the same as in Table 3.1

5.1.2 Joint Density Variation

In the next experiment, the densities of both the small cell tier and the macro tier were increased together, and the same metrics as before were measured. Table 5.2 contains the full parameters for this experiment.

Results. As with differential density, the biasing flips the effect the path loss model has on predicting to which tier the UE will connect. Figure 5.1 shows the fraction of users which connected to the small cell tier for different path loss models and densities, without any biasing and with a 20 dB bias. Note that, for each path loss model, the fraction of users associated with each tier remains the same with density, though the same 'flipping' trend is observed with biasing.

Next, as opposed to when the density of the small cells increased alone, the optimal bias values are independent of the densities of each tier varying together. Figure 5.8 shows the bias values that maximize the log sum rate. Due to the independent nature of these bias values, there is a constant gain from optimal biasing when compared to the no biasing case. Figure 5.9 shows probability of coverage as density increases. Note that the values with and without biasing do not converge, and there is always a gain with optimal biasing. Figure 5.10 shows a similar trend for log sum rate with optimal biasing.

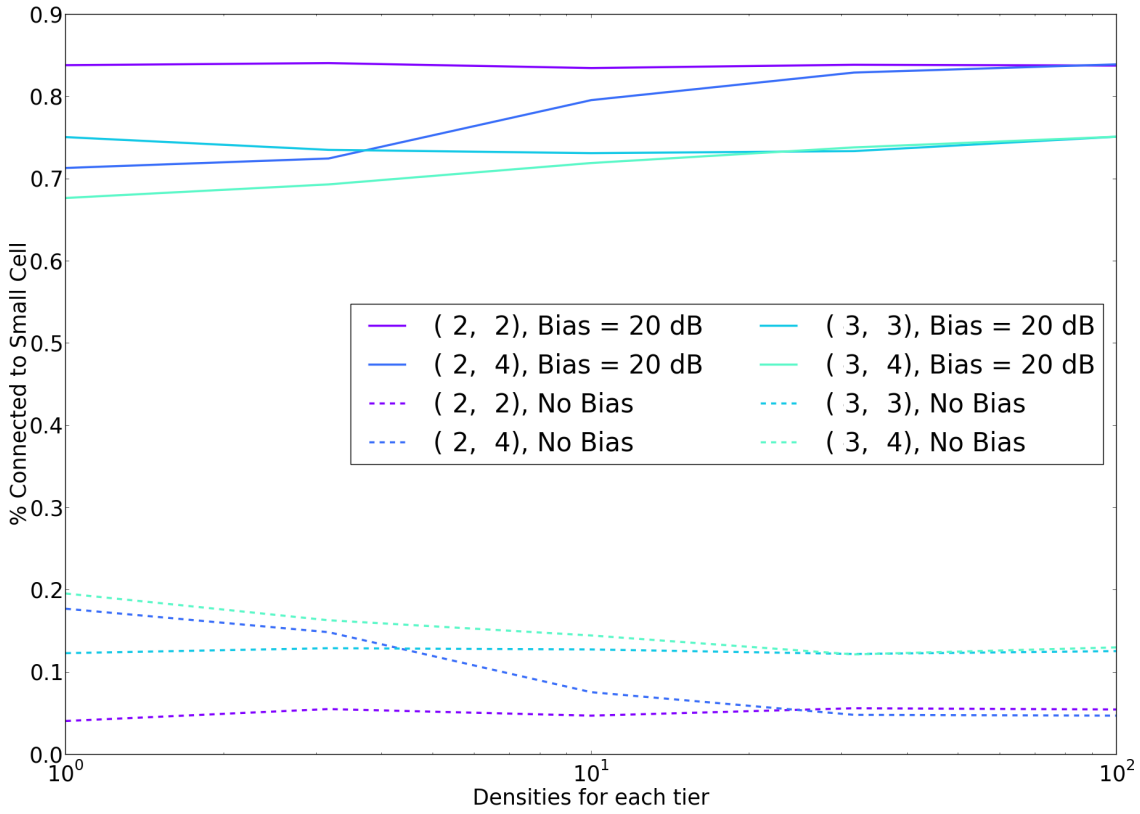

Figure 5.7: Fraction of UEs that connect to small cells as the density of both tiers increases

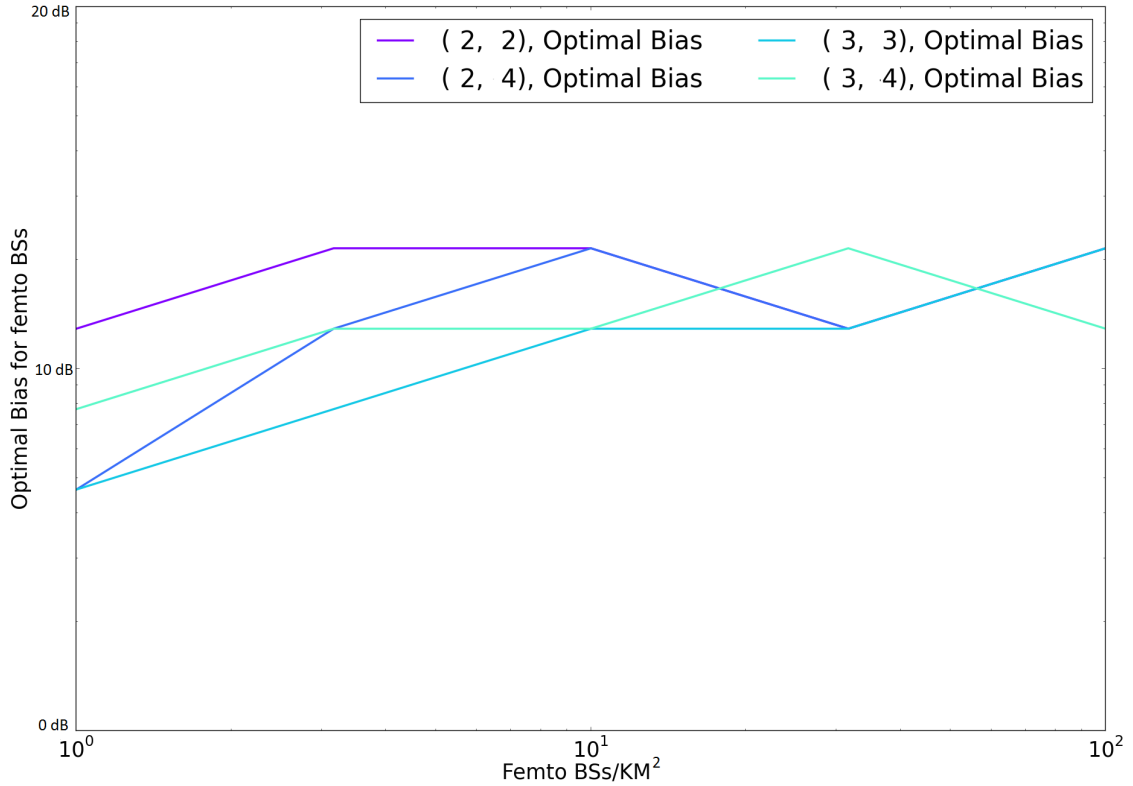

Figure 5.8: Optimal bias that maximizes the log sum rate as the densities of each tiers increase together.

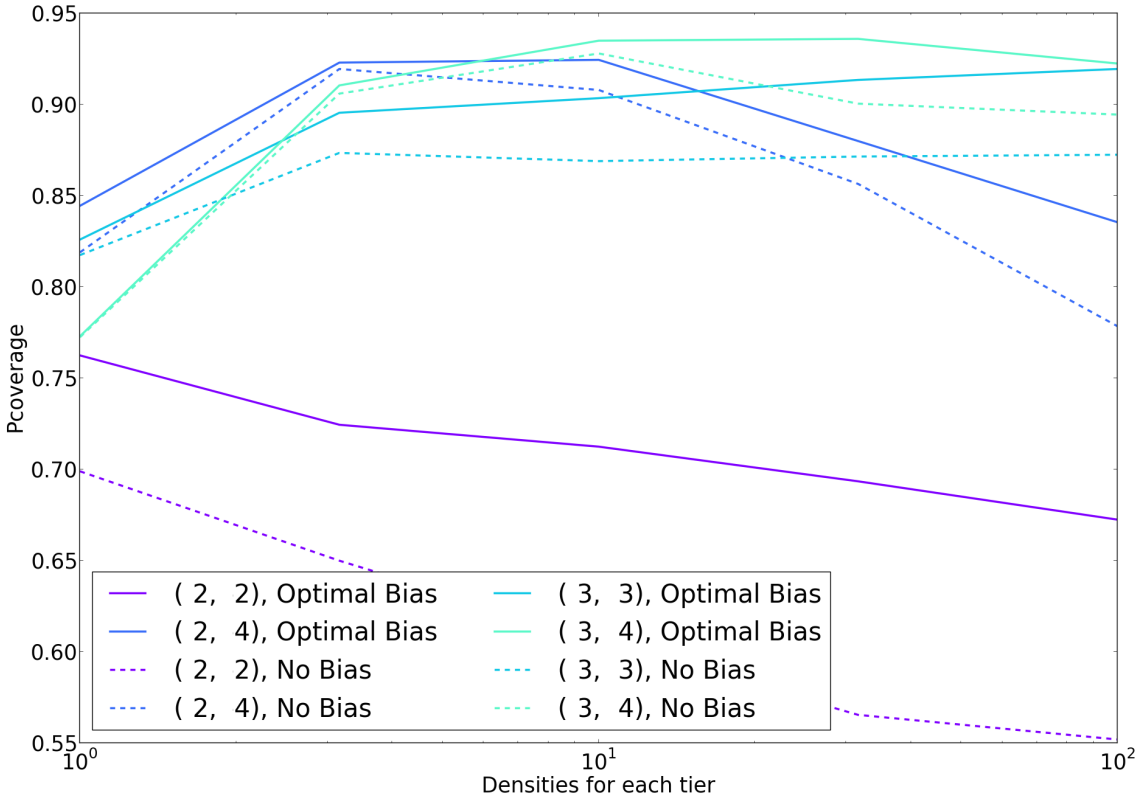

Figure 5.9: Probability of coverage with optimal biasing as the density of each tier increases.

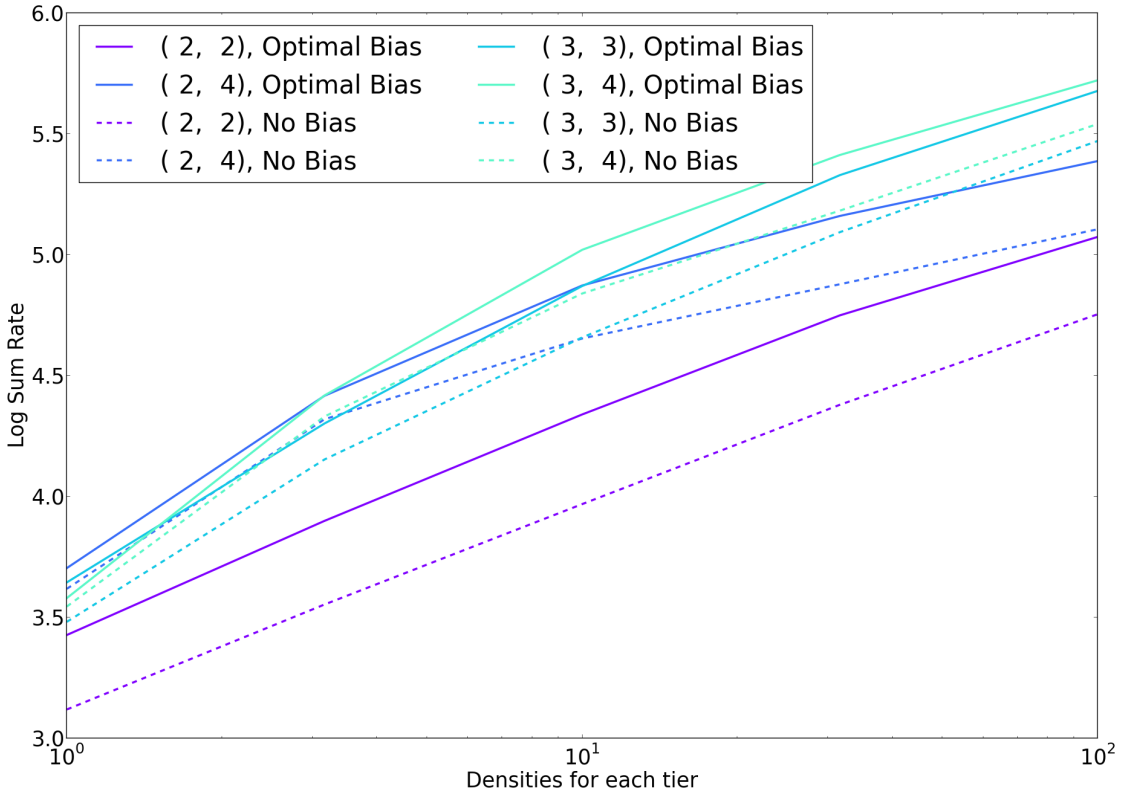

Figure 5.10: Log sum rate with optimal biasing as the density of each tier increases.

5.2 Uplink/Downlink Decoupling

With the same parameters as in the experiment described in Section 5.1.1, uplink association was decoupled from downlink association. Two forms of uplink association were studied: minimum path loss, as described in Section 3.3.2, and biasing for the uplink.

Results. Figures 5.11 and 5.12 show uplink log sum rate for decoupled association with UL Pathloss, decoupled association with optimal uplink biasing, and coupled association without biasing, and coupled association with optimal downlink biasing. As expected, biasing (toward small cells) for the uplink yields no gain. With uniform user and base station distributions, uplink load is evenly distributed and so biasing yields no benefit. However, decoupled association yields large gains over downlink association without biasing, as such association favors connections to macro base stations that may be further away than small cells. When biasing for the downlink, this gain is reduced about 50%, and decoupling yields a small but constant gain over optimal biasing for the downlink.

Finally, trends in tier association were measured for maximum biasing ($B_1 =$ 20 dB), optimal downlink biasing, uplink path loss, and downlink path loss. Figure 5.13 shows the trends as relative density increases. Note that, except for the $[\alpha_0, \alpha_1] = [2, 2]$ case, optimal biasing for the downlink is roughly halfway between uplink pathloss association and downlink association without biasing. This result suggests a downlink strategy that maximizes a linear combination of the downlink and uplink path losses. Such a strategy would approximately match the results of optimum static biasing – without the need to tune bias values. Future work may be implementing this proposed strategy and quantifying its loss against static biasing. Furthermore, the plots suggest why 20 dB biasing may never be the optimal strategy: it would often associate UEs to small cells that are further than the nearest macro cell.

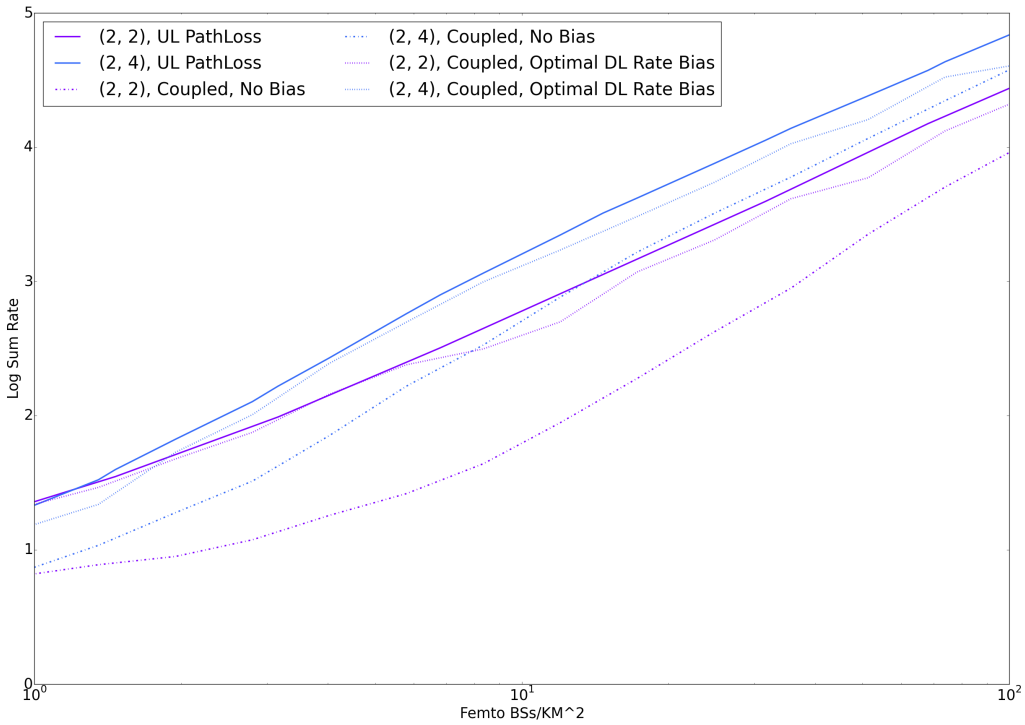

Figure 5.11: Uplink log sum rate with both coupled and decoupled association as relative density increases with $\alpha_0 = 2$

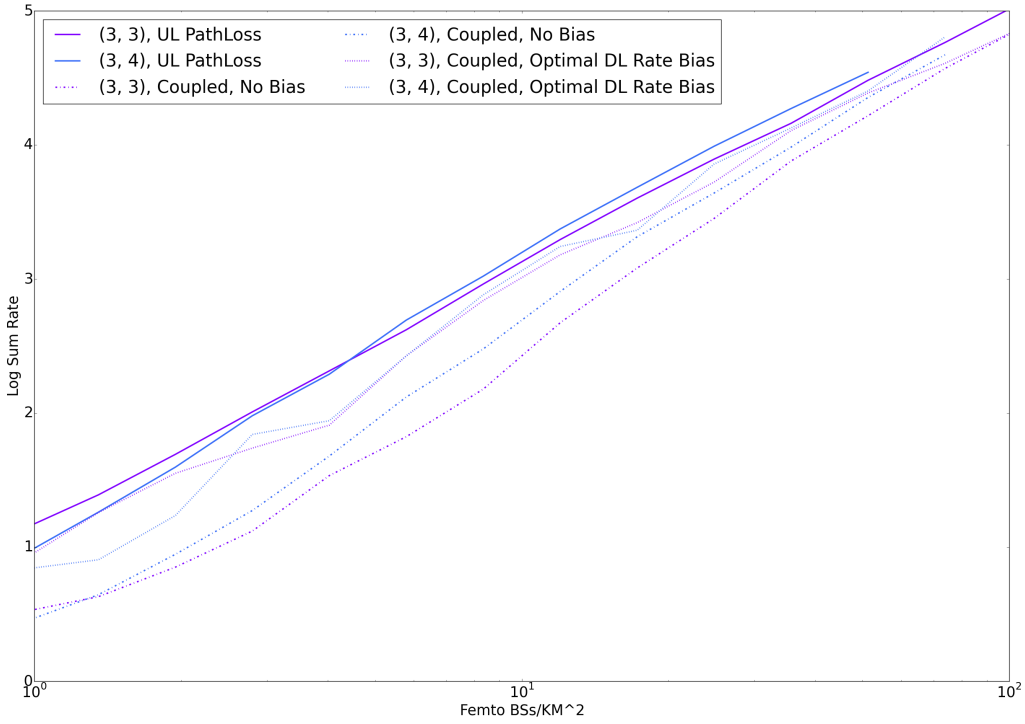

Figure 5.12: Uplink log sum rate with both coupled and decoupled association as relative density increases with $\alpha_0 = 3$

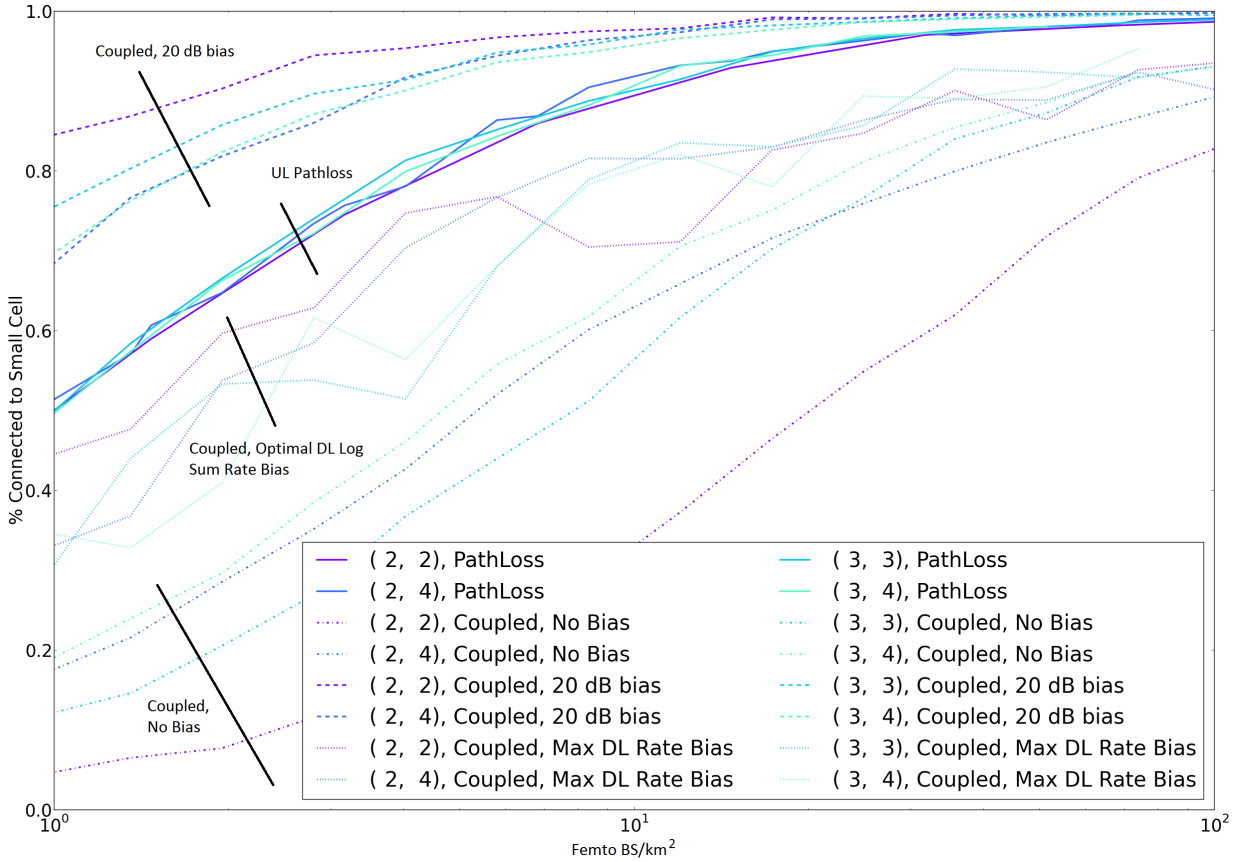

Figure 5.13: Comparison of fraction of UEs associated with small cell base stations for different association strategies

Chapter 6

Discussion and Conclusion

This thesis presents the use of a C++ simulator to analyze optimal biasing and uplink/downlink biasing under a stochastic geometry model. The 20x performance gains over a Matlab simulator is essential when running multi-day simulations with numerous parameter combinations, and the parallelizable nature of the code shows promise for future simulation work.

The simulator was used to study optimal biasing in two cases: with a density differential between tiers increasing and with the density of each tier increasing together. The optimal bias values and biasing gains is shown to be a function of the density ratio between the tiers. Future work can extend these methods to analyze to load balancing techniques and with changing power differentials.

Next, simulations were used to study uplink/downlink decoupling. Consistent with prior literature, there is a gain from associating the uplink separately (using path loss association). However, this gain is reduced 50% when optimal biasing for the downlink is used. This work can be extended by analyzing load balancing for both the uplink and the downlink.

These user association questions (for both the uplink and the downlink) must be answered for dense, next-generation networks. In order to support the applications

of tomorrow, next generations will be both dense and heterogeneous. Such networks must be managed correctly, and this thesis moves toward such answers. In future work, the insights gained from simulation will be specified analytically.

Bibliography

[1] "Cisco Visual Networking Index: Global Mobile Data Traffic Forecast Update 20142019 White Paper.".

[2] J. Andrews, S. Buzzi, W. Choi, S. Hanly, A. Lozano, A. Soong, and J. Zhang, "What Will 5g Be?," *IEEE Journal on Selected Areas in Communications*, vol. 32, pp. 1065–1082, June 2014.

[3] V. Chandrasekhar, J. G. Andrews, and A. Gatherer, "Femtocell networks: a survey," *Communications Magazine, IEEE*, vol. 46, no. 9, pp. 59–67, 2008.

[4] M. Dohler, R. W. Heath, A. Lozano, C. B. Papadias, and R. A. Valenzuela, "Is the PHY layer dead?," *Communications Magazine, IEEE*, vol. 49, no. 4, pp. 159–165, 2011.

[5] C. Shannon, "A Mathematical Theory of Communication," *Bell System Technical Journal*, vol. 27, pp. 379–423, 623–656, 1948.

[6] J. G. Andrews, F. Baccelli, and R. K. Ganti, "A Tractable Approach to Coverage and Rate in Cellular Networks," *IEEE Transactions on Communications*, vol. 59, pp. 3122–3134, Nov. 2011.

[7] X. Zhang and J. G. Andrews, "Downlink Cellular Network Analysis with Multi-slope Path Loss Models," *arXiv:1408.0549 [cs, math]*, Aug. 2014.

[8] A. Goldsmith, *Wireless Communications*. Cambridge ; New York: Cambridge University Press, 1 edition ed., Aug. 2005.

[9] International Telecommunication Union, *Yearbook of Statistics - Telecommunication/ICT Indicators - 2004-2013*. 40 ed., Dec. 2014.

[10] "Number of Cell Phones Worldwide Hits 4.6b.." Apr. 2010.

[11] C. Guglielmo, "Cisco Mobile Data Shows Surge in Smartphone Users, 4g Usage." Feb. 2013.

[12] A. Huurdeman, *The Worldwide History of Telecommunications*. A Wiley-interscience publication, Wiley, 2003.

[13] S. Johnston, "LTE Latency: How does it compare to other technologies?," Mar. 2014. http://opensignal.com/blog/2014/03/10/lte-latency-how-does-it-compare-to-other-technologies/.

[14] H. Moiin, "Expanding the human possibilities with 5g." Brooklyn 5G Summit, Apr. 2015.

[15] J. Gubbi, R. Buyya, S. Marusic, and M. Palaniswami, "Internet of Things (IoT): A vision, architectural elements, and future directions," *Future Generation Computer Systems*, vol. 29, pp. 1645–1660, Sept. 2013.

[16] "Nest." https://nest.com/.

[17] O. Kharif, "Cisco CEO Pegs Internet of Things as $19 Trillion Market." http://www.bloomberg.com/news/articles/2014-01-08/cisco-ceo-pegs-internet-of-things-as-19-trillion-market.

[18] "Google to acquire Nest for $3.2 billion." http://www.usatoday.com/story/tech/2014/01/13/google-to-acquire-nest-for-32-billion/4459879/.

[19] D. Miorandi, S. Sicari, F. De Pellegrini, and I. Chlamtac, "Internet of things: Vision, applications and research challenges," *Ad Hoc Networks*, vol. 10, pp. 1497–1516, Sept. 2012.

[20] L. Atzori, A. Iera, and G. Morabito, "The Internet of Things: A survey," *Computer Networks*, vol. 54, pp. 2787–2805, Oct. 2010.

[21] V. N. Swamy, S. Suri, P. Rigge, M. Weiner, G. Ranade, A. Sahai, and B. Nikolic, "Cooperative Communication for High-Reliability Low-Latency Wireless Control.".

[22] J. Harding, G. Powell, R. Yoon, J. Fikentscher, C. Doyle, D. Sade, M. Lukuc, J. Simons, and J. Wang, "Readiness of v2v technology for application," Tech. Rep. DOT HS 812 014, National Highway Traffic Safety Administration.

[23] K. Dresner and P. Stone, "Multiagent Traffic Management: A Reservation-Based Intersection Control Mechanism," in *The Third International Joint Conference on Autonomous Agents and Multiagent Systems*, pp. 530–537, July 2004.

[24] T. Parker, "Qualcomm's unlicensed LTE could crush carrier Wi-Fi's momentum.".

[25] "LTE Advanced in Unlicensed Spectrum.".

[26] J. Anon, "Qualcomm CTO Suggests LTE-U Will Not Be An Issue For Wi-Fi But Instead Will Be Beneficial To All | Androidheadlines.com.".

[27] "Unlicensed LTE could rock the mobile space in the coming years.".

[28] Y. Yiakoumis, M. Bansal, A. Covington, J. van Reijendam, S. Katti, and N. McKeown, "BeHop: a testbed for dense WiFi networks," pp. 1–8, ACM Press, 2014.

[29] H.-S. Jo, Y. J. Sang, P. Xia, and J. G. Andrews, "Heterogeneous cellular networks with flexible cell association: A comprehensive downlink SINR analysis," *IEEE Transactions on Wireless Communications*, vol. 11, no. 10, pp. 3484–3495, 2012.

[30] Y. Wang, S. Chen, H. Ji, and H. Zhang, "Load-aware dynamic biasing cell association in small cell networks," in *2014 IEEE International Conference on Communications (ICC)*, pp. 2684–2689, IEEE, 2014.

[31] Q. Ye, B. Rong, Y. Chen, M. Al-Shalash, C. Caramanis, and J. G. Andrews, "User association for load balancing in heterogeneous cellular networks," *IEEE Transactions on Wireless Communications*, vol. 12, no. 6, pp. 2706–2716, 2013.

[32] K. Smiljkovikj, P. Popovski, and L. Gavrilovska, "Analysis of the Decoupled Access for Downlink and Uplink in Wireless Heterogeneous Networks," *arXiv:1407.0536 [cs, math]*, July 2014.

[33] H. Elshaer, F. Boccardi, M. Dohler, and R. Irmer, "Downlink and uplink decoupling: a disruptive architectural design for 5g networks," *arXiv preprint arXiv:1405.1853*, 2014.

[34] S. Singh, X. Zhang, and J. G. Andrews, "Joint Rate and SINR Coverage Analysis for Decoupled Uplink-Downlink Biased Cell Associations in HetNets," *arXiv:1412.1898 [cs, math]*, Dec. 2014.

[35] F. Boccardi, J. Andrews, H. Elshaer, M. Dohler, S. Parkvall, P. Popovski, and S. Singh, "Why to Decouple the Uplink and Downlink in Cellular Networks and How To Do It," *arXiv preprint arXiv:1503.06746*, 2015.

[36] C.-H. Lee, C.-Y. Shih, and Y.-S. Chen, "Stochastic Geometry Based Models for Modeling Cellular Networks in Urban Areas," *Wirel. Netw.*, vol. 19, pp. 1063–1072, Aug. 2013.

[37] A. Guo and M. Haenggi, "Spatial Stochastic Models and Metrics for the Structure of Base Stations in Cellular Networks," *IEEE Transactions on Wireless Communications*, vol. 12, pp. 5800–5812, Nov. 2013.

Vita

Nikhil Garg is an undergraduate student in Electrical & Computer Engineering and Plan II Honors at the University of Texas at Austin. Nikhil's research interests are in modelling and design of heterogeneous wireless networks, along with policy questions related to wireless networks. He is also interested in machine learning and was part of a team that built a book recommendation engine. He has interned as a Software Engineer at Microsoft and as a Space Academy Research Associate at NASA Glenn Research Center. He also was a Next Generation Scholar at the Strauss Center for International Security and Law and served as a Legislative Intern at the Office of Texas State Senator Davis. Nikhil is an Eagle Scout, a Distinguished College Scholar of Engineering and Liberal Arts, and a recipient of the Unrestricted Endowed Presidential Scholarship at UT Austin. He also has been awarded an NSF Graduate Research Fellowship to support his PhD studies. In his spare time, Nikhil enjoys reading philosophy, working on coding projects, and being active in student societies.

Permanent address: nikhil_garg@utexas.edu

This thesis was typeset with LaTeX[†] by the author.

[†]LaTeX is a document preparation system developed by Leslie Lamport as a special version of Donald Knuth's TeX Program.